Modelling the multiple action pathways of projected climate change on the Pacific cod (*Gadus macrocephalus*) early life stages

Giancarlo M. Correa[1,2*], Thomas P. Hurst[3], William T. Stockhausen[4], Lorenzo Ciannelli[1], Trond Kristiansen[5,6], Darren J. Pilcher[7,8]

[1]College of Earth, Ocean, and Atmospheric Sciences, Oregon State University, Corvallis, OR, USA

[2]School of Aquatic and Fishery Sciences, University of Washington, Seattle, WA, USA

[3]National Marine Fisheries Service, National Oceanic and Atmospheric Administration, Alaska Fisheries Science Center, Newport, OR, USA

[4]National Marine Fisheries Service, National Oceanic and Atmospheric Administration, Alaska Fisheries Science Center, Seattle, WA, USA

[5]Farallon Institute, Petaluma, CA, USA

[6]Norwegian Institute for Water Research (NIVA), Oslo, Norway

[7]Cooperative Institute for Climate, Ocean, and Ecosystem Studies, University of Washington, Seattle, WA, USA

[8]Pacific Marine Environmental Laboratory, National Oceanic and Atmospheric Administration, Seattle, WA, USA

*Corresponding author. Email: g.moroncorrea@gmail.com

Abstract

Understanding how future ocean conditions will impact early life stages and population recruitment of fishes is critical for adapting fisheries communities to climate change. In this study, we incorporated projected changes in physical and biological ecosystem dynamics from an oceanographic model into a mechanistic individual-based model for larval and juvenile stages of the Pacific cod (*Gadus macrocephalus*) in the eastern Bering Sea. We particularly investigated the impacts of ocean currents, temperature, prey density, and pCO2 on the hatching success, growth, survival, and spatial distribution of this species during 2021-2100. We evaluated two CO_2 emission scenarios: RCP8.5 (high CO_2 emissions, low mitigation efforts) and RCP4.5 (medium CO_2 emissions and mitigation efforts). We found that the increase in temperature and decrease in prey density were the main drivers of faster growth rates and lower survival through increased starvation by the end of the century. Conversely, pCO_2 had negligible impacts, which suggests that this species might be resilient to ocean acidification. The largest effects were observed under the high CO_2 emission scenario, while the RCP4.5 projections displayed minimal impacts. We also identified an area with favourable conditions in the southeastern Bering Sea that will likely persist in future decades. This study provides relevant information on the future impacts of climate change on Pacific cod, and our results can be used to implement and inform climate-ready management for this important stock in Alaska.

Keywords: climate change, Pacific cod, fish, ocean acidification, individual-based modelling

1. Introduction

In the last century, anthropogenic greenhouse gas emissions (e.g., CO_2) to the atmosphere, driven principally by human fossil fuel combustion, have played a key role in modulating the world's climate (IPCC, 2021). The ocean absorbs more than 25% of anthropogenic CO_2 production, changing the ocean's carbonate chemistry and altering fundamental chemical balances by a process known as ocean acidification (OA, Doney et al., 2009). The ocean also absorbs, redistributes, and stores heat on long timescales, which has produced a rise in ocean temperatures in the last decades (Cheng et al., 2019). OA and warming are known as the 'evil twins' of marine climate change (Nagelkerken et al., 2016), and both can alter the ocean environment and the species living therein in numerous ways. Some current effects of climate change on marine organisms include disruption in shell formation and physiological development, reduced somatic growth, habitat modification, and spatial distribution shifts (Cattano et al., 2020, 2018; Doney et al., 2009; Kleisner et al., 2017; Nagelkerken and Munday, 2016). These impacts may be aggravated in the future because ocean temperatures and CO_2 are predicted to rise even more rapidly during the present century (Meinshausen et al., 2011).

The response of the early life stages of fish to the environment is essential for recruitment, a primary driver of the abundance of a fish population (Duffy-Anderson et al., 2005). Fish larvae are especially susceptible to climate change (Dahlke et al., 2020; Koenigstein et al., 2016), where the impacts can be grouped into direct – those affecting the biology and behaviour of individuals - and indirect - via ecosystem processes - effects (Nagelkerken et al., 2016; Nagelkerken and Munday, 2016; Ottersen et al., 2010). Literature on the direct impacts of ocean warming on fish larvae is extensive, reporting changes in metabolism, growth, and development (Deutsch et al., 2015; Pinsky et al., 2013). Historically, fish were assumed to be resilient to ocean acidification through active ion transport (Kroeker et al., 2013); nevertheless, during the last decade, studies have demonstrated that acid-base regulation influences fish calcification, behaviour, and ion transport, affecting physiology and development, primarily during early life stages as they lack specialized internal pH regulatory mechanisms (Cattano et al., 2018). In addition to these direct effects, indirect effects may alter linked ecosystem processes. For example, increases in temperature and reductions in ocean pH may result in increased mortality of copepods (Cripps et al., 2014) and altered fatty acid composition (Garzke et al., 2016) of key prey species. A warmer ocean also alters heat content and currents (Mueter and Litzow, 2008; Munday et al., 2009), which may further impact larval behaviour and transport (Fuchs et al., 2020). These multiple action pathways modulate the overall impact of climate conditions on larvae ecology (Cominassi et al., 2020).

The Bering Sea is an ecosystem that has experienced changes in climate conditions in the last decades (Stabeno et al., 2017). This ecosystem supports a wide diversity of fish species, large-scale commercial fisheries representing 40% of the U.S. commercial catch, and small coastal fishing communities that depend on subsistence harvest (Haynie and Huntington, 2016). Pacific cod (*Gadus macrocephalus*) is a keystone species in the Bering Sea food web; it dwells on the continental shelves from the Sea of Japan across the North Pacific Rim to the California coast (West et al., 2020). The impacts of climate change on the ecology of this species are already being observed. For example, recent warming events have produced a northward movement of Pacific cod in the Bering Sea (Barbeaux and Hollowed, 2018; Stevenson and Lauth, 2019). Moreover,

recent studies have reported changes in the prey field available to Pacific cod larvae, with higher dominance of small and less lipid-rich zooplankton taxa during warm years (Coyle et al., 2008; Kimmel and Duffy-Anderson, 2020). Warming might also increase the relative risk of a trophic mismatch of cod larvae with their primary food sources and trigger poor recruitment in Alaska, as observed in recent years (Laurel et al., 2021). There is also evidence that ocean acidification may impact the Pacific cod larval growth (Hurst et al., 2019) and survival of its congeners (Stiasny et al., 2016), associated with impairments in physiological functioning and morphological development (Frommel et al., 2012; Hurst et al., 2021; Stiasny et al., 2019).

Large biophysical changes are predicted to occur in the future to the Bering Sea ecosystem (Hermann et al., 2019, 2016). Due to a warmer environment, large zooplankton taxa are expected to be less abundant on the outer shelf (Hermann et al., 2019). The southward advection of ice, critical for this ecosystem, is projected to decrease with winds becoming more northward, in turn contributing to warmer areas in the south (Hermann et al., 2019). The Bering Sea is also particularly vulnerable to ocean acidification since high-latitude waters are already naturally low in carbonate ion concentrations, which can buffer the effect of increased CO_2 dissolution (Cross et al., 2014; Fabry et al., 2009). High CO_2 emissions scenarios predicted for the future may produce a pH average decrease of 0.3 to 0.4 units in the ocean, an unprecedented level in the last few centuries (IPCC, 2021). A few studies have already evaluated the future impacts of climate change on the larval ecology of marine species of economic importance in the Bering Sea, suggesting a decrease in recruitment and fisheries revenues and profits for some crab species (Punt et al., 2016; Szuwalski et al., 2021) and walleye pollock (*Gadus chalcogrammus*) (Mueter et al., 2011). Similar results were found for several stocks of the Atlantic cod (*Gadus morhua*) in the North Atlantic (Kristiansen et al., 2014). However, to date, no effort has been made to examine the cumulative and interactive effects of the multiple action pathways by which climate change may affect the ecology of Pacific cod's early life stages.

In this study, we used model projections of the Bering Sea ecosystem until the end of the century (2021 - 2100) under two CO_2 emission scenarios to investigate the direct and indirect impacts of future climate conditions on the Pacific cod's early life stages. We primarily focus on the effects of warming, prey abundance, and ocean acidification. To accomplish our goals, we used an individual-based model (IBM), previously applied to this species in this ecosystem (Correa et al., 2024) and in the Gulf of Alaska (Hinckley et al., 2019), to mechanistically model the impacts of the environment on fish ecology based on published evidence. We evaluated future changes in (1) the environment experienced by fish, (2) hatching success, (3) growth, (4) survival, and (5) spatial distribution. Understanding the extent to which cod is susceptible to climate change is of high management, economic, and social interest since Pacific cod is the second most harvested species in the Bering Sea (Haynie and Huntington, 2016). More broadly, our model and findings can be incorporated into future studies that evaluate the multiple action pathways of climate change on early life stages of fish and project population abundance, catches, and profit.

2. Materials and methods

This study combined projected changes in physical and biological ecosystem dynamics with an IBM to evaluate their impacts on larval and juvenile stages of Pacific cod over the period 2021 – 2100. The IBM was initially developed by Hinckley et al. (2019), with the addition of a foraging sub-model (Correa et al., 2024). A summary of each component is provided below. For more details on the IBM, see Correa et al. (2024).

2.1. Study region

The EBS is situated between the Arctic Ocean and the North Pacific and is characterized by a broad (>500 km) and shallow (<100 m) shelf (Figure 1). The shelf has three biophysical domains: (1) a vertically well-mixed inner shelf domain (~0 – 50 m depth), (2) a middle shelf domain that is well-mixed in winter but strongly stratified in summer (~50 – 100 m depth), and (3) an outer shelf domain more gradually stratified (~100 – 200 m depth) (Kachel et al., 2002). The Alaska Coastal Current and the Alaskan Stream enter the Bering Sea through passes in the Aleutian Island chain and flow northward along the inner shelf and the slope (Stabeno et al., 2016). Ice formed each winter in the northern Bering Sea is advected to the southeast, where it melts as it interacts with warmer water (Hermann et al., 2019). The ice extent and timing of retreat vary annually, being a major physical feature that influences community composition and species distribution in this ecosystem (Mueter and Litzow, 2008). The EBS stands out because of its high productivity, supported by nutrient-rich waters from the North Pacific Ocean and replenishment of nitrate, phosphate, and silicate from deep waters to the shelf (Stabeno et al., 2001). High nutrient levels trigger high primary productivity, which supports zooplankton populations, demersal and pelagic fishes, top-predators, and numerous commercial fisheries (Aydin and Mueter, 2007).

2.2. Simulating future oceanographic conditions

We used the earth system models: Geophysical Fluid Dynamics Laboratory Earth System Model 2M (GFDL, Dunne et al., 2012), the National Center for Atmospheric Research Community Earth System Model (CESM, Kay et al., 2015), and the Model for Interdisciplinary Research on Climate (MIROC, Watanabe et al., 2011); all of them selected from the Climate Model Intercomparison Project phase 5 (CMIP-5) (Taylor et al., 2012). The earth system models were driven with two representative concentration pathways (Moss et al., 2010) from the IPCC Fifth Assessment Report (IPCC, 2021) that describe different trajectories for future greenhouse gas emissions, mitigation, and subsequent climate change: RCP8.5 and RCP4.5. The former scenario represents an unmitigated pathway with high greenhouse emissions (also known as the 'business as usual' scenario), and the latter is an intermediate scenario that assumes the imposition of emissions mitigation policies. CESM (RCP4.5) projections were only available until 2079.

We used the regional model Bering10K, thoroughly described in Hermann et al. (2016) and Kearney et al. (2020). This regional model is based on the Regional Ocean Modeling System (ROMS), which is a modelling system for developing time-varying, three-dimensional (3D) regional ocean circulation models (Haidvogel et al., 2008; Shchepetkin and McWilliams, 2005). The Bering10K model is driven at the sea surface and lateral ocean boundaries by variables from the coarse resolution global earth system model to achieve a dynamic downscaling (Hermann et al., 2019). The Bering10K regional grid has ~10km spatial horizontal resolution with 30 vertical layers, and the domain spans the Bering Sea and the northern Gulf of Alaska. The Bering10K model also includes the carbonate chemistry dynamics, with values of pCO_2, ocean pH, and aragonite saturation (Pilcher et al., 2022, 2019). The model is coupled to a nutrient-phytoplankton-zooplankton model (BESTNPZ) to simulate the lower-trophic-level ecosystem (Gibson and Spitz, 2011; Hermann et al., 2016; Kearney et al., 2020). Four prey categories in the form of bulk zooplankton carbon ($mg\ C.m^{-3}$) are modelled, which were then partitioned into size categories using a relative size-frequency distribution of zooplankton (Daewel et al., 2007; Kristiansen et al., 2011). The model output was saved at a weekly temporal resolution but temporally interpolated within the IBM to obtain a daily resolution.

2.3.Individual-based model

DisMELS is an IBM framework written in the Java programming language (Arnold et al., 2005) previously used to study dispersal mechanisms for the larvae of fish stocks in Alaska (Cooper et al., 2013; Gibson et al., 2019; Hinckley et al., 2019; Stockhausen et al., 2019b, 2019a); including the Pacific cod in the EBS (Correa et al., 2024). The base model used in this study is described in Hinckley et al. (2019) and Correa et al. (2024). The main variables and equations are described in Tables 1 and 2.

Pacific cod in the EBS spawn in the winter along the outer shelf break and along the Aleutian Islands (Neidetcher et al., 2014). Eggs are demersal and are rarely sampled during ichthyoplankton surveys. After hatching, yolk-sac larvae move to the surface and remain there during their early life stages (Hurst et al., 2009). Unlike Pacific cod in the Gulf of Alaska, Pacific cod in the EBS do not settle during their first six months after hatching and are found across the broad shelf in both demersal and pelagic trawl surveys (Hurst et al., 2012). The transition timing between distinct stages (see below) is principally temperature-dependent.

Five life stages were included in the IBM: egg, yolk-sac larvae, pre-flexion larvae, post-flexion larvae, and epipelagic juvenile. Particles were released yearly from 206 spawning locations (Figure 1, Neidetcher et al., 2014) every seven days during March and tracked until September 15 (~ six months). Here, the term 'particle' is the model unit, so each particle will have a standard length, dry weight, hatching success, and state (see Section 2.3.2) associated with it for every model time step. However, given the term 'particle' is mostly used in physical applications, we will use the term 'fish' for simplicity hereafter, acknowledging that one 'fish' in the IBM might represent the features and behaviour of one fish, ten fish, or one million fish in the field.

Eggs were released on the ocean bottom (~100 and 300 m depth) and remained in the same location until hatching. Embryonic growth, egg stage duration, and hatching success were a function of temperature (Equations 1-4; Hurst et al., 2010; Laurel et al., 2008; Laurel and Rogers, 2020). Upon hatching, yolk-sac larvae migrated to the surface waters (Doyle and Mier, 2016; Hurst et al., 2009) with vertical velocity $10^{-4}\ m/s$ (Hinckley et al., 2019). The number of days to complete the absorption of the yolk sac and growth (when the yolk sac was present) was a function of temperature (Equations 5 and 7; Hurst et al., 2010; Laurel et al., 2011, 2008). After the yolk-sac absorption (YSA), larval growth was modelled as described in the bioenergetic section (see Section 2.3.1). The number of days to reach the point of no return following YSA (PNR, when a larva cannot recover from starvation, Equation 6) was temperature-dependent with an exponentially decreasing shape (Laurel et al., 2011, 2008). If a larva ingested prey before the PNR, it transitioned to the pre-flexion stage. During the pre-flexion stage, larvae moved vertically between 0 and 60 m depth (Equation 10; Hurst et al., 2009). Larvae transitioned to the post-flexion larval stage when their standard length (L) reached 13.5 mm. Diel vertical migration was initiated in this stage with daytime depths of 30-60 m and nighttime depths of 0 and 30 m (Hurst et al., 2015, 2009). When larvae reached a standard length of 25 mm, they passed to the epipelagic juvenile stage.

2.3.1. Feeding and growth

In this section, we briefly describe the bioenergetic model used for larval and juvenile growth after yolk-sac absorption.

We modelled the number of prey items encountered and ingested for each time step. The feeding efficiency of fish is highly dependent on reactive distance (Equation 11), which is a function of the light intensity in the environment. Light intensity was calculated based on depth, time of day, and chlorophyll (Fiksen et al., 2002). Encounter rate ($enc, prey. s^{-1}$) was estimated on the ability of fish to visually perceive the prey and formulated for pause-travel searchers (i.e., search for prey only while pausing between swimming events) such as cod species (Equation 12, Aksnes and Giske, 1993; Aksnes and Utne, 1997; Fiksen et al., 2002; Fiksen and MacKenzie, 2002; MacKenzie and Kiørboe, 1995). Once prey is located within the field of perception, the fish moves to the attack position. The probability of attack success (PCA) when $L < 17\ mm$ was modelled as described in Fiksen and MacKenzie (2002) (Equation 13) and when $L \geq 17\ mm$ as in Daewel et al. (2011) (formulated for larger larvae and juveniles, Equation 14).

Ingested prey biomass (Equation 16) was added to the food biomass already in the gut. If the larva consumed enough food to grow at the physiological maximum, the growth was restricted by temperature alone (Folkvord, 2005). In such circumstances, the instantaneous growth rate in weight (g, d^{-1}) for non-egg stages depended on temperature ($T, °C$) and dry weight ($w,\ mg$) (Equation 7, Hurst et al., 2010). If stomach content (S_t, mg, Equation 19) was lower than the food biomass in the gut required to grow at the physiological maximum (D_{max}, Equation 18), growth was food-limited and constrained by the food in the stomach (Kristiansen et al., 2014, 2009, 2007). The available food biomass in the stomach at the current time-step (S_t, mg) was a function of the ingested material (ing), the remaining stomach content from the previous time-step (S_{t-1}, mg), and the food biomass used for growth, respiration, and loss to egestion ($D \in [0, D_{max}], mg$).

Then, the fish dry weight at time step t (w_t, mg) was calculated through increases from prey digestion and decreases from metabolized energy (Equations 20-22). The standard length (L_t) was estimated from dry weight based on an observed length-weight relationship collected in different experiments (Figure S1; Equation 8; Hurst et al., 2019, 2010).

2.3.2. Fish state

We distinguish two fish states in every model time step: surviving or dead. A fish was considered dead if it starved or its final location (to September 15) was out of the EBS. Starvation occurred under two conditions: 1) reaching the PNR, or 2) when the body mass calculated at any time step was 75% or less of the potential body mass (exclusively temperature-dependent) at the corresponding time step (accounting for poor body condition) (Peck and Hufnagl, 2012). Dead fish were only tracked until the last time step considered 'surviving' and then excluded from the IBM. Our analyses used the percentage of surviving fish within a year or location as a metric of survival.

2.4. Climate change impacts

This study focuses on the direct and indirect impacts of future ocean conditions, with a special focus on temperature, prey density, and ocean acidification, on the ecology of Pacific cod's early life stages. The impacts of temperature and prey density are explicitly accounted for in the IBM; however, the impacts of OA have been omitted from the IBM thus far. While there is evidence of OA effects on a wide range of marine taxa, the impacts on lower trophic levels (i.e., prey fields) or Pacific cod biology have not been sufficiently described to warrant model parameterization. Therefore, we incorporated a range of generalized responses that describe the multiple action pathways by which changes in pCO_2 concentration may impact the biology of the studied species.

These were based on experimental studies of marine zooplankton, Pacific cod, and its congeners. The referenced laboratory experiments generally contrasted responses between low-pCO_2 (~400-500 μatm) and high-pCO_2 treatments (~1000-1500 μatm). Based on the responses observed, for each variable described below, we identified a plausible magnitude of the effect that would be expected to occur over CO_2 levels from 500 to 1500 μatm, and assumed a linear response between these endpoints (Figure S2). The incorporated responses are detailed below and were applied at each model time step.

Metabolism

Metabolism was a function of temperature as formulated in our model; however, OA has also been reported to increase the metabolic rates in Atlantic cod, likely due to higher larval energetic demands produced by a high CO_2 concentration in the environment (Dahlke et al., 2017). Based on the findings of Dahlke et al. (2017), we increased the active metabolism (M_a, Equation 21) as a function of pCO_2 by a maximum of 10% (direct effect).

Growth

Laboratory studies that examined the impacts of OA on the somatic growth of cod larvae have shown divergent responses. High levels of CO_2 were observed to decrease growth rates during the first two weeks after hatching and then increase during the subsequent three weeks (Hurst et al., 2019). Conversely, Frommel et al. (2013) found no differences in the standard length of pre-feeding Baltic cod larvae under different levels of pCO_2, while Frommel et al. (2012) only found slightly larger sizes of Atlantic cod at 32 and 39 days post-hatching (dph) under high pCO_2 treatments. Based on results observed for Pacific cod larvae (Hurst et al. 2019), we reduced the calculated growth rate by a maximum of 10% as a function of pCO_2 concentration during the first two weeks after hatching and then increased it by a maximum of 15% within the subsequent three weeks (direct effect).

Probability of capture success (PCA)

High CO_2 might impact the first feeding of cod larvae (Stiasny et al., 2016). For example, the swim bladder inflation rate of walleye pollock larvae was negatively affected by high CO_2 treatments (Hurst et al., 2021), which might lead to less successful feeding (Czesny et al., 2005) and potentially affect long-term survival (Woolley and Qin, 2010). Because there is no quantification of the impacts of OA on the feeding behaviour of gadids in the EBS, we assumed a reduction in the probability of attack success (PCA) as a function of pCO_2 concentration by a maximum of 10% (direct effect).

Prey abundance

Evidence suggests that copepods are generally resilient to OA, concluded from studies focused on adult stages during short-term exposure to high levels of pCO_2 (Campoy et al., 2020; Wang et al., 2018). However, this response might be stage- and species-specific. For example, pCO_2 levels higher than 1000 μatm may increase the mortality of early life stages (nauplii) of some zooplankton through disturbance in energy allocation, which may act as bottlenecks and then decrease the recruitment and population abundance (Cripps et al., 2016, 2014; Lewis et al., 2013). McLaskey et al. (2016) found negative effects of OA on krill larval development and survival in the North Pacific. Also, the interaction of OA with other variables, such as thermal stress or food limitation, might aggravate the overall impacts (Wang et al., 2018). Based on a review of the

effects of OA on several copepod species (Wang et al., 2018), we decreased the total zooplankton abundance as a function of pCO_2 concentration by a maximum of 10% (indirect effect).

Prey quality

Temperature and OA may reduce body size of copepods (Garzke et al., 2016; Vehmaa et al., 2016) by changing energy allocation between growth and defence against unfavourable environmental conditions (Wang et al., 2018). This effect might be exacerbated if food becomes scarce (Escribano and McLaren, 1992), as it is predicted to be in the Bering Sea in future years (Hermann et al., 2019). Also, the amount of fatty acid in prey, crucial for good fish condition (Copeman and Laurel, 2010), might be impacted in some species (McLaskey et al., 2019), which may decrease the prey quality for fish larvae. To simulate these two effects in our model, we reduced the prey's individual weight (Huebert and Peck, 2014) as a function of pCO_2 by a maximum of 10% (Wang et al., 2018) (indirect effect).

2.5.Analysis of results

We analysed changes in the average environmental conditions (temperature, pCO_2, and prey density) experienced by fish through larval and juvenile stages (see Figure S3). We evaluated temporal changes in the percentage of fish that survived to September 15, and then dead fish were removed from the subsequent analyses. We evaluated changes in the following biological variables: (1) hatching success (indicates the probability of successful hatching), (2) standard length to September 15, and (3) growth performance. Growth performance is the ratio between the potential maximum dry weight (exclusively temperature-dependent) and the realized dry weight (temperature and food-dependent). A growth performance value equal to 1 means that growth has not been limited by prey in the environment.

Temporal variations were explored by plotting the distribution of variables among fish by CO_2 emission scenario, oceanographic model, and decade. To explore spatiotemporal variation, the temporal trend at each initial (i.e., release) location (Figure 1) was explored by using the slope ($beta$) of the linear model:

$$bio_{var} = alpha_z + beta_z * year$$

Where bio_{var} represents the variable (either environmental or biological) and z indicates an initial location. A positive or negative $beta$ indicates that values at the initial location z increase or decrease over the years, respectively. These values were analysed by emission scenario, and information among oceanographic models was combined. Finally, changes in spatial distribution were evaluated by comparing density maps of final locations by emission scenario and decade.

Table S2 shows the different model runs (i.e., combinations of Earth system model, emission scenario, and assumed OA effects) examined in this study. Our main results assume that the OA effects occur simultaneously on the five biological components described in the previous section. However, we also aimed to examine the OA effects independently in order to explore their influence on our results as a sensitivity analysis. This exploration was done only for the last decade (2090-2100) when the highest pCO_2 is projected and, therefore, the largest effects are expected to occur. A second sensitivity analysis explored how temperature, prey density, and light intensity modulate the impacts of pCO_2 on Pacific cod. To do so, we ran the IBM with constant environmental conditions and no movement during the fish lifespan, evaluating different values of temperature (from 0 to 10℃), prey density (a factor multiplies a standard vector of prey densities:

Euphausiids = 5.5 mgC/m^3, On-shelf large-bodied copepods = 1.5 mgC/m^3, Off-shelf large-bodied copepods = 1 mgC/m^3, Small-bodied copepods = 4 mgC/m^3), light intensity (light-limited vs. high light intensity), and pCO_2 (high -1500 μatm- vs. low -500 μatm- conditions) on the fish standard length and the number of days to die from starvation. This second sensitivity analysis does not aim to represent any particular environmental scenario but to explore how different environmental variables interact and identify the conditions where the effect of OA would be the largest.

The IBM was run on a laptop Intel Core i9-9880H with 32GB RAM. The analyses of the IBM outputs were performed in R (R Core Team, 2022). The code to process the IBM outputs can be found at: https://github.com/GiancarloMCorrea/PcodIBM_EBS_forecast.

3. Results

Changes in the environment

For the RCP8.5 scenario, Pacific cod experienced an environment that warmed and increased in pCO_2 steadily between 2021 and 2100 (Figure 2). Comparing the initial and final analyzed decade, we observed an increase in temperature (°C) between 43% and 85% among oceanographic models, while pCO_2 increased up to ~100%. The RCP4.5 scenario did not display a clear temporal trend: temperature increased ~16% for the MIROC and CESM but not for the GFDL model, and pCO_2 increased ~15%. Generally, we observed that the MIROC oceanographic model produced higher pCO_2 values and warmer temperatures for both scenarios, while the GFDL displayed the smallest changes over decades. Median euphausiids and small-bodied copepods density in the cod habitat decreased by ~15% by 2100, especially for the MIROC model, under the RCP8.5 emission scenario (Figure 3). On the other hand, we did not detect significant changes in large-bodied copepods' density. The RCP4.5 scenario did not display substantial changes in prey density.

We observed that the increase in temperature and pCO_2 was less severe and uniform across release locations for the RCP4.5 scenario (Figure S4). For the RCP8.5 scenario, the increase in temperature was more rapid on the middle and inner shelves. In contrast, the increase in pCO_2 displayed the opposite pattern, exhibiting a rapid increase on the outer shelf. For prey density, minor temporal trends were observed for the RCP4.5 scenario across release locations for all prey items (Figure S5). Under the RCP8.5 scenario, densities of small-bodied copepods and euphausiids encountered decreased across all the cod release locations, especially on the outer shelf, whereas large-bodied copepods increased on the inner shelf but decreased on the outer shelf.

Changes in survival

The percentage of fish that remained in the EBS to September 15 was consistent over the decades for both scenarios (Figure 4). Under the MIROC model, a few fish (~1%) were transported out of the EBS domain, while ~7% of fish were advected out of the system under the GFDL and CESM models. Fish with a higher probability of being advected out of the EBS were those released on the northern portion of the outer shelf (Figure 5). Under the RCP4.5 scenario, the percentage of fish that survived starvation remained ~70-80% and did not display a temporal trend. Conversely, a large decline was observed for the RCP8.5 scenario: -83% for MIROC, -25% for CESM, and -8% for GFDL. We found that fish that died from starvation were released mainly on the outer shelf for both emission scenarios but also on the middle shelf for the RCP8.5 scenario. Moreover, starvation generally occurred in deep areas (> 200 m depth) with limited light irradiance (Figure S6).

Changes in biological variables

The temporal and spatiotemporal variability in biological features were reported only for surviving fish. Hatching success fluctuated between 0.2 and 0.4 across decades for all emission scenarios and models (Figure 6). MIROC (RCP8.5) was the only case that showed a clear negative temporal trend. Hatch success decreased on the middle and outer shelf for the RCP4.5 scenario (Figure 7) and increased across several release locations for the RCP8.5 scenario.

For RCP4.5, the CESM model predicted an increase in standard length to September 15 over decades (+ ~15% by the end of the century), but no temporal trend was observed under MIROC or GFDL. Conversely, all models showed an increase between 10% and 20% in standard length for the RCP8.5 scenario. The MIROC and CESM models predicted the largest resulting fish sizes and a reduction in length variability over time. Spatial trends showed that fish increased in size most rapidly under the RCP8.5 scenario and on the middle and inner shelf.

Median growth performance was always higher than 95% and remained constant over decades for both scenarios; however, there was a reduction in variance over time, a pattern that was clearer for the RCP8.5 scenario (Figure 6). Temporal trends by release locations displayed stronger and positive trends for fish released on the outer shelf and negative but weaker trends for fish released on the middle and inner shelf (Figure 7).

Changes in the spatial distribution

Final locations showed that fish generally were not advected far from their release locations. The highest fish density was observed in the southern margin of the Bering Sea consistently over the modelled period and for both emission scenarios (Figures 8 and S7). This pattern was consistent among the Earth System models as well. Secondary areas of concentration occurred on the middle shelf. While the overall density of survivors decreased over time under the RCP8.5, especially on the middle shelf, there were no marked shifts in the overall distribution of surviving juveniles.

Impacts of ocean acidification

We found that the incorporated effects of OA had negligible impacts on Pacific cod's growth and survival (Figures S8 and S9). The first sensitivity analysis, which compared the impacts of individual and cumulative effects described in Section 2.4, displayed no significant differences in the percentage of surviving fish, standard length, and growth performance from the baseline scenario (when no OA effects were assumed). The second sensitivity analysis, which analysed suites of environmental conditions, showed that a high pCO_2 concentration would decrease the time to starvation only in a constant light-limited environment. This impact would be exacerbated by an increase in temperature and a decrease in prey density (Figure S10). On the other hand, the standard length of surviving fish did not vary between low and high pCO_2 treatments regardless of the other environmental variables (Figure S11).

4. Discussion

Using a modelling approach, we investigated how projected climate change scenarios may impact the ecology of the Pacific cod's early life stages in the EBS. We found that the increase in temperature and decrease in prey density were the main drivers of the observed changes in growth and survival, while the effects of OA, either combined or independently, had only minimal impacts on the biological metrics in our study. The magnitude of this impact varied by oceanographic

model, but we generally found that a warmer habitat under the RCP8.5 scenario could decrease the percentage of fish surviving starvation between ~8% and ~83% and increase the standard length of surviving fish up to 20%. Conversely, no clear temporal trend in any analysed variable was identified under the RCP4.5 scenario, which suggests that Pacific cod early life stages may not be impacted under these lower CO_2 emission conditions. The previously identified retention area in the southeastern Bering Sea (Correa et al., 2024) is expected to persist in the future, offering a suitable habitat for cod larvae and juveniles. Our study provides useful information on potential changes in larval survival and growth over space and time, which could be incorporated into fisheries management and adaptation decisions to climate change in this region. Moreover, this study provides a framework for incorporating results from fish-related OA laboratory experiments in IBMs that might be applied to other species.

Hermann et al. (2021, 2019) did a complete description of the projected biophysical conditions of the Bering Sea up to 2100 using the Bering10K model. Under the RCP8.5 scenario, they reported an increase of as much as ~4 and ~3 ℃ in surface and bottom temperature, respectively, especially on the middle and inner shelf of the northern Bering Sea. Also, they predict a reduction in ice cover and biomass of phytoplankton, small-bodied copepods, and euphausiids, especially on the middle and outer shelf of the southern Bering Sea. Using the Bering10K model and CMIP5 projections, Pilcher et al. (2022) predict a decrease in pH and the aragonite saturation state and an increase in pCO_2 under the high-emission scenario in the Bering Sea, which will have a negative impact on calcifying organisms. In this study, we examined the environmental conditions in the locations where Pacific cod dwelled from spawning through their first summer of life. Under the RCP8.5 scenario, we also project a substantial increase in temperature (~ 2-3 ℃) and pCO_2 (~ 400 μatm) and a reduction in small-bodied copepods and euphausiid density, two critical prey items for the Pacific cod's early life stages. However, we did not notice significant temporal trends in any environmental variable under the RCP4.5 scenario despite their effects being predicted to be approximately half as intense as those expected under the high-emission scenario in the entire Bering Sea (Hermann et al., 2019).

Correa et al. (2024) found temperature as a critical factor in modulating starvation for Pacific cod in the EBS. Moreover, they found moderate evidence of a negative effect of temperature on annual recruitment. They concluded that a warmer environment accelerates the yolk sac consumption and the need for larvae to obtain food from their environment. Given that this species spawns on the ocean bottom, newly hatched larvae need to reach the surface, where ideal conditions for successful exogenous feeding can be found, as quickly as possible. However, a rapid yolk sac absorption caused by a warmer environment may force larvae to search for prey in deeper areas, where prey density is low and light is limited. We found that the rise in temperature in the cod habitat under the RCP8.5 scenario might reduce the survival and recruitment through increased starvation, particularly for larvae hatched on deeper areas of the outer and middle shelf of the EBS. Despite the three oceanographic models predicting a reduction in surviving fish, the reduction level was quite variable (from 8% to 83%). The potential decrease in recruitment under the RCP8.5 scenario can trigger a cascading effect, decreasing the population abundance and, therefore, catches and profits, as also predicted for walleye pollock in this ecosystem (Mueter et al., 2011). Future studies could include our predictions in population dynamics and bioeconomic models to quantify this cascading effect (e.g., Punt et al., 2016).

Larger juvenile fish sizes are expected to be more frequent under a warmer environment in future years, principally due to the increase in growth rates but also due to larger larvae size-at-hatch and

low survival of slow-growing fish. Moreover, the increase in fish size under the high-emission scenario means that surviving fish could cope with the adverse conditions by finding suitable habitats. The southeastern Bering Sea was identified as a retention area by Correa et al. (2024). In our study, we observed that this area with high fish density persisted regardless of the emission scenario. This area also had the smallest reduction in important prey items under the high-emission emission scenario, shallow depth (< ~150 m), and low starvation frequency. The persistence of this retention area in future years has relevant management implications since it could act as a larval refuge and source under potential future adverse conditions. Conversely, the reduction in the density of juveniles on the outer shelf over the decades under the high-emission scenario suggests that this region may be the most affected.

Model-based estimates of prey density in the Pacific cod larval and juvenile habitat did not display large variations from 2000 to 2020 (Correa et al., 2024), and their effects on growth and survival were assumed to be secondary compared to temperature during this period. However, the relevance of prey density on fish survival may become more significant in future years under the high-emission scenario (Hermann et al., 2019). Due to their size and quality, small-bodied copepods (*Pseudocalanus* sp.) are critical prey for a successful transition from endogenous to exogenous feeding for gadids, as supported by field data (Bailey et al., 1995). Under the RCP8.5 scenario, their expected decrease in abundance in the Bering Sea, especially on the outer shelf (Hermann et al., 2019), may interact with the warmer environment and, therefore, contribute to the increase in starvation after yolk-sac absorption in the future (Figure 9). The reduction of this prey item is predicted to happen predominantly on the outer shelf; therefore, larvae hatched in this area might be mostly affected. The projected decline in euphausiids did not impact the growth of surviving fish since the growth performance index became larger during the last decades, meaning that their growth was not food-limited.

As we described previously, several laboratory studies have aimed to investigate the impacts of OA on diverse aspects of the biology of gadids in Alaska (T. Hurst et al., 2012; Hurst et al., 2021, 2019, 2013). Laboratory studies are useful since they can isolate individual effects of independent variables on a response variable. However, it is difficult to extrapolate laboratory results to the field since early life stages occur in a constantly fluctuating environment, being impacted by several environmental variables simultaneously. To our knowledge, this is the first study that integrates diverse effects, both directly upon physiology and indirectly via changes in prey availability, from OA into an IBM for fish. This gives us the advantage of modelling multiple pathways of OA effects on larval and juvenile fish. Here, we observed no significant overall impact of OA on fish size, growth performance, and survival. There are a couple of main reasons that could explain this result. First, OA is less important than temperature and prey density in determining fish growth and survival, with its impacts on survival being masked by these more important variables. Second, the median pCO_2 concentration in the cod habitat was found to be generally ~1000 μatm by the end of the century in the most extreme scenario, which is lower than the level used in laboratory experiments on larval sensitivity (~1500 μatm; Hurst et al., 2019). In addition, the linear interpolation between low and high pCO_2 levels might underestimate the OA effects at intermediate pCO_2 concentrations.

OA can also affect the biological aspects of larvae and juvenile fish that have yet to be examined in the Pacific cod. For example, high pCO_2 level affects the calcification of otoliths for Atlantic cod larvae (Maneja et al., 2013), potentially leading to changes in orientation and movement. Hatch success might also be affected, as observed for Atlantic cod (Dahlke et al., 2017). There is

evidence that high levels of pCO_2 could also increase the incidence of morphological deformities for Atlantic cod larvae (Dahlke et al., 2017; Frommel et al., 2012), which might decrease the survival probability and recruitment (Stiasny et al., 2016). However, even for the same species, the response of gadids to changes in pCO_2 levels could be ecosystem- (Frommel et al., 2013) and stage-specific (Cattano et al., 2018). Additionally, more research is needed to understand the impacts of OA on copepods and euphausiids in the Bering Sea, the main prey of the early life stages of fish. Hare et al. (2007) found that high pCO_2 concentrations might provoke a shift in the phytoplankton community in the Bering Sea, which could impact zooplankton dynamics. While some studies suggest that non-calcifying organisms in the Bering Sea may be resilient to OA (Mathis et al., 2015), more laboratory experiments are required to evaluate such effects for inclusion in this modelling framework.

Our IBM included several important aspects of the Pacific cod's early life stages; however, there are some features that need to be accounted for in future studies, such as spatial variations in egg density, changes in the parental stock, egg mortality, and prey quality. Spawning sites (i.e., release locations) were considered uniform over time in our study; however, the Pacific cod's spatial distribution is already being affected by rapid warming in the Bering Sea (Baker, 2021; Spies et al., 2020; Stevenson and Lauth, 2019). Using species distribution models, Rooper et al. (2021) predict that adult Pacific cod is not expected to move the centre of gravity of their distribution in future years but may expand their area occupied. However, these studies focus on the average distribution during summer, which could largely differ from the spawning areas during late winter (Neidetcher et al., 2014). Bigman et al. (2023) predict an expansion of the Pacific cod spawning habitat towards shallower and more northern areas in the EBS, especially under a high-emission scenario. An inshore movement of spawning sites would benefit the survival of yolk-sac larvae since they would reach surface waters quicker, finding ideal conditions for exogenous feeding and counteracting the negative effects of a warmer environment.

In the field, the number of eggs produced every spawning season is a function of the spawning biomass: more and larger females generate more and larger eggs (Hixon et al., 2014). In our model, we assumed a constant number of eggs released throughout the forecast period, which implicitly assumes that the spawning biomass remains constant. By projecting ecosystem dynamics at the base of the food web, Whitehouse et al. (2021) estimated a reduction in the total biomass of Pacific cod in the Bering Sea for both RCP4.5 and RCP8.5 scenarios in future years. A reduction in spawning biomass might intensify the decrease in survival predicted in this study. In addition, Whitehouse et al. (2021) also project an increase in jellyfish, an important predator of fish larvae in the EBS (Brodeur et al., 2008), by 2100, which could negatively affect the cod larval survival. Finally, small-bodied copepods and euphausiids are considered high-quality prey for Pacific cod (Farley et al., 2016), and their projected decrease in abundance will affect not only the prey ingestion rates (in grams) but also the energy and essential fatty acids (EFAs) intake. EFAs are an important source of energy for gadids in Artic and sub-Artic waters and can modulate their growth and survival (Copeman and Laurel, 2010). Future research might consider quantifying the energy content in the prey items, their expected changes, and their impacts on the growth and survival of Pacific cod larvae under climate change.

Conclusions

This study uses a model-based approach to study the impacts of climate change on the early life stages of the Pacific cod in the EBS. We provide new insights about the direct and indirect impacts

of future changes in temperature, prey density, and OA on cod larvae and juveniles. Under the high CO_2 emission scenario (RCP8.5), this study predicts an increase in the standard length of Pacific cod juveniles by increasing the growth rates of surviving fish. Moreover, starvation is expected to be more frequent, producing a decrease in survival during the first days after hatching, especially for fish hatched in deeper areas on the middle and outer shelf of the EBS. The temperature is the main variable driving changes in growth and survival, and the decrease in prey density may exacerbate the negative impacts of the high-emission scenario. While more laboratory studies are necessary to understand the full impact of OA on diverse aspects of the Pacific cod biology, we have not found any cumulative impact of OA on Bering Sea Pacific cod length and survival in response to the sensitivities described to date. We suggest the use of this framework for the evaluation of multifactor climate effects on Bering Sea fish populations, communities, and fisheries under climate change.

Declaration of Competing Interest

The authors declare that they have no known competing financial interests or personal relationships that could have appeared to influence the work reported in this paper.

Acknowledgements

We thank Cheryl Barnes and the two anonymous reviewers for providing valuable comments on an earlier version of this manuscript. We also thank NOAA's Alaska Integrated Assessment Program (IEA) and the Alaska Climate Integrated Modeling Project (ACLIM) for providing outputs of the high-resolution downscaled ROMSNPZ projections for the Bering Sea. Giancarlo M. Correa was funded by a grant from NOAA's Ocean Acidification Program to TPH. This publication is partially funded by the Cooperative Institute for Climate, Ocean, & Ecosystem Studies (CICOES) under NOAA Cooperative Agreement NA20OAR4320271, Contribution No. 2023-1288. This is PMEL contribution No. 5516 and Eco-FOCI contribution No. 1056.

Authorship contribution statement

Giancarlo M. Correa: Conceptualization, methodology, formal analysis, Writing – Original draft. **Thomas P. Hurst**: Conceptualization. Writing – review and editing. **William T. Stockhausen**: Methodology. Software. Writing – review and editing. **Lorenzo Ciannelli**: Conceptualization. Writing – review and editing. **Trond Kristiansen**: Methodology. Writing – review and editing. **Darren J. Pilcher**: Methodology. Writing – review and editing.

References

Aksnes, D.L., Giske, J., 1993. A theoretical model of aquatic visual feeding. Ecological Modelling 67, 233–250. https://doi.org/10.1016/0304-3800(93)90007-F

Aksnes, D.L., Utne, A.C.W., 1997. A revised model of visual range in fish. Sarsia 82, 137–147. https://doi.org/10.1080/00364827.1997.10413647

Arnold, K., Gosling, J., Holmes, D., 2005. The Java programming language. Addison Wesley Professional.

Aydin, K., Mueter, F., 2007. The Bering Sea—A dynamic food web perspective. Deep Sea Research Part II: Topical Studies in Oceanography 54, 2501–2525. https://doi.org/10.1016/j.dsr2.2007.08.022

Bailey, K., Canino, M., Napp, J., Spring, S., Brown, A., 1995. Contrasting years of prey levels, feeding conditions and mortality of larval walleye pollock Theragra chalcogramma in the western Gulf of Alaska. Mar. Ecol. Prog. Ser. 119, 11–23. https://doi.org/10.3354/meps119011

Baker, M.R., 2021. Contrast of warm and cold phases in the Bering Sea to understand spatial distributions of Arctic and sub-Arctic gadids. Polar Biol 44, 1083–1105. https://doi.org/10.1007/s00300-021-02856-x

Barbeaux, S.J., Hollowed, A.B., 2018. Ontogeny matters: Climate variability and effects on fish distribution in the eastern Bering Sea. Fish Oceanogr 27, 1–15. https://doi.org/10.1111/fog.12229

Bigman, J.S., Laurel, B.J., Kearney, K., Hermann, A.J., Cheng, W., Holsman, K.K., Rogers, L.A., 2023. Predicting Pacific cod thermal spawning habitat in a changing climate. ICES Journal of Marine Science fsad096. https://doi.org/10.1093/icesjms/fsad096

Brodeur, R.D., Decker, M.B., Ciannelli, L., Purcell, J.E., Bond, N.A., Stabeno, P.J., Acuna, E., Hunt, G.L., 2008. Rise and fall of jellyfish in the eastern Bering Sea in relation to climate regime shifts. Progress in Oceanography 77, 103–111. https://doi.org/10.1016/j.pocean.2008.03.017

Campoy, A.N., Cruz, J., Ramos, J.B.E., Viveiros, F., Range, P., Alexandra Teodósio, M., 2020. Ocean Acidification Impacts on Zooplankton, in: Teodósio, M.A., Barbosa, A.B. (Eds.), Zooplankton Ecology. CRC Press, First. | Boca Raton: CRC Press, [2021], pp. 64–82. https://doi.org/10.1201/9781351021821-5

Cattano, C., Agostini, S., Harvey, B.P., Wada, S., Quattrocchi, F., Turco, G., Inaba, K., Hall-Spencer, J.M., Milazzo, M., 2020. Changes in fish communities due to benthic habitat shifts under ocean acidification conditions. Science of The Total Environment 725, 138501. https://doi.org/10.1016/j.scitotenv.2020.138501

Cattano, C., Claudet, J., Domenici, P., Milazzo, M., 2018. Living in a high CO2 world: a global meta-analysis shows multiple trait-mediated fish responses to ocean acidification. Ecol Monogr 88, 320–335. https://doi.org/10.1002/ecm.1297

Cheng, L., Abraham, J., Hausfather, Z., Trenberth, K.E., 2019. How fast are the oceans warming? Science 363, 128–129. https://doi.org/10.1126/science.aav7619

Cominassi, L., Moyano, M., Claireaux, G., Howald, S., Mark, F.C., Zambonino-Infante, J.-L., Peck, M.A., 2020. Food availability modulates the combined effects of ocean acidification and warming on fish growth. Sci Rep 10, 2338. https://doi.org/10.1038/s41598-020-58846-2

Cooper, D.W., Duffy-Anderson, J.T., Stockhausen, W.T., Cheng, W., 2013. Modeled connectivity between northern rock sole (Lepidopsetta polyxystra) spawning and nursery areas in the eastern Bering Sea. Journal of Sea Research 84, 2–12. https://doi.org/10.1016/j.seares.2012.07.001

Copeman, L.A., Laurel, B.J., 2010. Experimental evidence of fatty acid limited growth and survival in Pacific cod larvae. Mar. Ecol. Prog. Ser. 412, 259–272. https://doi.org/10.3354/meps08661

636 Correa, G.M., Hurst, T.P., Stockhausen, W.T., Ciannelli, L., Kristiansen, T., Pilcher, D.J., 2024. Modeling
637 the larval growth and survival of Pacific cod (Gadus macrocephalus) in the eastern Bering Sea. Progress
638 in Oceanography 225, 103282. https://doi.org/10.1016/j.pocean.2024.103282

639 Coyle, K.O., Pinchuk, A.I., Eisner, L.B., Napp, J.M., 2008. Zooplankton species composition, abundance
640 and biomass on the eastern Bering Sea shelf during summer: The potential role of water-column
641 stability and nutrients in structuring the zooplankton community. Deep Sea Research Part II: Topical
642 Studies in Oceanography 55, 1775–1791. https://doi.org/10.1016/j.dsr2.2008.04.029

643 Cripps, G., Flynn, K.J., Lindeque, P.K., 2016. Ocean Acidification Affects the Phyto-Zoo Plankton Trophic
644 Transfer Efficiency. PLoS ONE 11, e0151739. https://doi.org/10.1371/journal.pone.0151739

645 Cripps, G., Lindeque, P., Flynn, K.J., 2014. Have we been underestimating the effects of ocean
646 acidification in zooplankton? Glob Change Biol 20, 3377–3385. https://doi.org/10.1111/gcb.12582

647 Cross, J.N., Mathis, J.T., Lomas, M.W., Moran, S.B., Baumann, M.S., Shull, D.H., Mordy, C.W., Ostendorf,
648 M.L., Bates, N.R., Stabeno, P.J., 2014. Integrated assessment of the carbon budget in the southeastern
649 Bering Sea. Deep Sea Research Part II: Topical Studies in Oceanography 109, 112–124.

650 Czesny, S.J., Graeb, B.D.S., Dettmers, J.M., 2005. Ecological Consequences of Swim Bladder Noninflation
651 for Larval Yellow Perch. Transactions of the American Fisheries Society 134, 1011–1020.
652 https://doi.org/10.1577/T04-016.1

653 Daewel, U., Peck, M.A., Schrum, C., 2011. Life history strategy and impacts of environmental variability
654 on early life stages of two marine fishes in the North Sea: an individual-based modelling approach.
655 Canadian Journal of Fisheries and Aquatic Sciences 68, 426–443. https://doi.org/10.1139/F10-164

656 Daewel, U., Peck, M.A., Schrum, C., St John, M.A., 2007. How best to include the effects of climate-
657 driven forcing on prey fields in larval fish individual-based models. Journal of Plankton Research 30, 1–5.
658 https://doi.org/10.1093/plankt/fbm094

659 Dahlke, F.T., Leo, E., Mark, F.C., Pörtner, H., Bickmeyer, U., Frickenhaus, S., Storch, D., 2017. Effects of
660 ocean acidification increase embryonic sensitivity to thermal extremes in Atlantic cod, Gadus morhua.
661 Glob Change Biol 23, 1499–1510. https://doi.org/10.1111/gcb.13527

662 Dahlke, F.T., Wohlrab, S., Butzin, M., Pörtner, H.-O., 2020. Thermal bottlenecks in the life cycle define
663 climate vulnerability of fish. Science 369, 65–70. https://doi.org/10.1126/science.aaz3658

664 Deutsch, C., Ferrel, A., Seibel, B., Pörtner, H.-O., Huey, R.B., 2015. Climate change tightens a metabolic
665 constraint on marine habitats. Science 348, 1132–1135. https://doi.org/10.1126/science.aaa1605

666 Doney, S.C., Fabry, V.J., Feely, R.A., Kleypas, J.A., 2009. Ocean Acidification: The Other CO2 Problem.
667 Annu. Rev. Mar. Sci. 1, 169–192. https://doi.org/10.1146/annurev.marine.010908.163834

668 Doyle, M.J., Mier, K.L., 2016. Early life history pelagic exposure profiles of selected commercially
669 important fish species in the Gulf of Alaska. Deep Sea Research Part II: Topical Studies in Oceanography
670 132, 162–193. https://doi.org/10.1016/j.dsr2.2015.06.019

671 Duffy-Anderson, J.T., Bailey, K., Ciannelli, L., Cury, P., Belgrano, A., Stenseth, N.Chr., 2005. Phase
672 transitions in marine fish recruitment processes. Ecological Complexity 2, 205–218.
673 https://doi.org/10.1016/j.ecocom.2004.12.002

674 Dunne, J.P., John, J.G., Adcroft, A.J., Griffies, S.M., Hallberg, R.W., Shevliakova, E., Stouffer, R.J., Cooke,
675 W., Dunne, K.A., Harrison, M.J., Krasting, J.P., Malyshev, S.L., Milly, P.C.D., Phillipps, P.J., Sentman, L.T.,
676 Samuels, B.L., Spelman, M.J., Winton, M., Wittenberg, A.T., Zadeh, N., 2012. GFDL's ESM2 Global
677 Coupled Climate–Carbon Earth System Models. Part I: Physical Formulation and Baseline Simulation
678 Characteristics. Journal of Climate 25, 6646–6665. https://doi.org/10.1175/JCLI-D-11-00560.1

679 Escribano, R., McLaren, I.A., 1992. Influence of food and temperature on lengths and weights of two
680 marine copepods. J. Exp. Mar. Biol. Ecol. 159, 77–88.

681 Fabry, V.J., McClintock, J.B., Mathis, J.T., Grebmeier, J.M., 2009. Ocean acidification at high latitudes: the
682 bellwether. Oceanography 22, 160–171. https://doi.org/10.5670/oceanog.2009.105

683 Farley, E.V., Heintz, R.A., Andrews, A.G., Hurst, T.P., 2016. Size, diet, and condition of age-0 Pacific cod
684 (Gadus macrocephalus) during warm and cool climate states in the eastern Bering sea. Deep Sea
685 Research Part II: Topical Studies in Oceanography 134, 247–254.
686 https://doi.org/10.1016/j.dsr2.2014.12.011

687 Fiksen, Ø., Aksnes, D.L., Flyum, M.H., Giske, J., 2002. The influence of turbidity on growth and survival of
688 fish larvae: a numerical analysis. Hydrobiologia 484, 49–59. https://doi.org/10.1023/A:1021396719733

689 Fiksen, Ø., MacKenzie, B., 2002. Process-based models of feeding and prey selection in larval fish.
690 Marine Ecology Progress Series 243, 151–164. https://doi.org/10.3354/meps243151

691 Folkvord, A., 2005. Comparison of size-at-age of larval Atlantic cod (Gadus morhua) from different
692 populations based on size- and temperature-dependent growth models. Canadian Journal of Fisheries
693 and Aquatic Sciences 62, 1037–1052. https://doi.org/10.1139/f05-008

694 Frommel, A.Y., Maneja, R., Lowe, D., Malzahn, A.M., Geffen, A.J., Folkvord, A., Piatkowski, U., Reusch,
695 T.B.H., Clemmesen, C., 2012. Severe tissue damage in Atlantic cod larvae under increasing ocean
696 acidification. Nature Clim Change 2, 42–46. https://doi.org/10.1038/nclimate1324

697 Frommel, A.Y., Schubert, A., Piatkowski, U., Clemmesen, C., 2013. Egg and early larval stages of Baltic
698 cod, Gadus morhua, are robust to high levels of ocean acidification. Mar Biol 160, 1825–1834.
699 https://doi.org/10.1007/s00227-011-1876-3

700 Fuchs, H.L., Chant, R.J., Hunter, E.J., Curchitser, E.N., Gerbi, G.P., Chen, E.Y., 2020. Wrong-way migrations
701 of benthic species driven by ocean warming and larval transport. Nat. Clim. Chang. 10, 1052–1056.
702 https://doi.org/10.1038/s41558-020-0894-x

703 Garzke, J., Hansen, T., Ismar, S.M.H., Sommer, U., 2016. Combined Effects of Ocean Warming and
704 Acidification on Copepod Abundance, Body Size and Fatty Acid Content. PLoS ONE 11, e0155952.
705 https://doi.org/10.1371/journal.pone.0155952

706 Gibson, G.A., Spitz, Y.H., 2011. Impacts of biological parameterization, initial conditions, and
707 environmental forcing on parameter sensitivity and uncertainty in a marine ecosystem model for the
708 Bering Sea. Journal of Marine Systems 88, 214–231. https://doi.org/10.1016/j.jmarsys.2011.04.008

Gibson, G.A., Stockhausen, W.T., Coyle, K.O., Hinckley, S., Parada, C., Hermann, A.J., Doyle, M., Ladd, C., 2019. An individual-based model for sablefish: Exploring the connectivity between potential spawning and nursery grounds in the Gulf of Alaska. Deep Sea Research Part II: Topical Studies in Oceanography 165, 89–112. https://doi.org/10.1016/j.dsr2.2018.05.015

Haidvogel, D.B., Arango, H., Budgell, W.P., Cornuelle, B.D., Curchitser, E., Di Lorenzo, E., Fennel, K., Geyer, W.R., Hermann, A.J., Lanerolle, L., Levin, J., McWilliams, J.C., Miller, A.J., Moore, A.M., Powell, T.M., Shchepetkin, A.F., Sherwood, C.R., Signell, R.P., Warner, J.C., Wilkin, J., 2008. Ocean forecasting in terrain-following coordinates: Formulation and skill assessment of the Regional Ocean Modeling System. Journal of Computational Physics 227, 3595–3624. https://doi.org/10.1016/j.jcp.2007.06.016

Hare, C., Leblanc, K., DiTullio, G., Kudela, R., Zhang, Y., Lee, P., Riseman, S., Hutchins, D., 2007. Consequences of increased temperature and CO2 for phytoplankton community structure in the Bering Sea. Mar. Ecol. Prog. Ser. 352, 9–16. https://doi.org/10.3354/meps07182

Haynie, A.C., Huntington, H.P., 2016. Strong connections, loose coupling: the influence of the Bering Sea ecosystem on commercial fisheries and subsistence harvests in Alaska. E&S 21, art6. https://doi.org/10.5751/ES-08729-210406

Hermann, A.J., Gibson, G.A., Bond, N.A., Curchitser, E.N., Hedstrom, K., Cheng, W., Wang, M., Cokelet, E.D., Stabeno, P.J., Aydin, K., 2016. Projected future biophysical states of the Bering Sea. Deep Sea Research Part II: Topical Studies in Oceanography 134, 30–47. https://doi.org/10.1016/j.dsr2.2015.11.001

Hermann, A.J., Gibson, G.A., Cheng, W., Ortiz, I., Aydin, K., Wang, M., Hollowed, A.B., Holsman, K.K., 2019. Projected biophysical conditions of the Bering Sea to 2100 under multiple emission scenarios. ICES Journal of Marine Science fsz043. https://doi.org/10.1093/icesjms/fsz043

Hermann, A.J., Kearney, K., Cheng, W., Pilcher, D., Aydin, K., Holsman, K.K., Hollowed, A.B., 2021. Coupled modes of projected regional change in the Bering Sea from a dynamically downscaling model under CMIP6 forcing. Deep Sea Research Part II: Topical Studies in Oceanography 194, 104974. https://doi.org/10.1016/j.dsr2.2021.104974

Hinckley, S., Stockhausen, W.T., Coyle, K.O., Laurel, B.J., Gibson, G.A., Parada, C., Hermann, A.J., Doyle, M.J., Hurst, T.P., Punt, A.E., Ladd, C., 2019. Connectivity between spawning and nursery areas for Pacific cod (Gadus macrocephalus) in the Gulf of Alaska. Deep Sea Research Part II: Topical Studies in Oceanography 165, 113–126. https://doi.org/10.1016/j.dsr2.2019.05.007

Hixon, M.A., Johnson, D.W., Sogard, S.M., 2014. BOFFFFs: on the importance of conserving old-growth age structure in fishery populations. ICES Journal of Marine Science 71, 2171–2185. https://doi.org/10.1093/icesjms/fst200

Huebert, K.B., Peck, M.A., 2014. A Day in the Life of Fish Larvae: Modeling Foraging and Growth Using Quirks. PLoS ONE 9, e98205. https://doi.org/10.1371/journal.pone.0098205

Hurst, T., Fernandez, E., Mathis, J., Miller, J., Stinson, C., Ahgeak, E., 2012. Resiliency of juvenile walleye pollock to projected levels of ocean acidification. Aquat. Biol. 17, 247–259. https://doi.org/10.3354/ab00483

747 Hurst, T.P., Cooper, D.W., Duffy-Anderson, J.T., Farley, E.V., 2015. Contrasting coastal and shelf nursery
748 habitats of Pacific cod in the southeastern Bering Sea. ICES Journal of Marine Science 72, 515–527.
749 https://doi.org/10.1093/icesjms/fsu141

750 Hurst, T.P., Cooper, D.W., Scheingross, J.S., Seale, E.M., Laurel, B.J., Spencer, M.L., 2009. Effects of
751 ontogeny, temperature, and light on vertical movements of larval Pacific cod (*Gadus macrocephalus*).
752 Fisheries Oceanography 18, 301–311. https://doi.org/10.1111/j.1365-2419.2009.00512.x

753 Hurst, T.P., Copeman, L.A., Andrade, J.F., Stowell, M.A., Al-Samarrie, C.E., Sanders, J.L., Kent, M.L., 2021.
754 Expanding evaluation of ocean acidification responses in a marine gadid: elevated CO2 impacts
755 development, but not size of larval walleye pollock. Mar Biol 168, 119. https://doi.org/10.1007/s00227-
756 021-03924-w

757 Hurst, T.P., Copeman, L.A., Haines, S.A., Meredith, S.D., Daniels, K., Hubbard, K.M., 2019. Elevated CO2
758 alters behavior, growth, and lipid composition of Pacific cod larvae. Marine Environmental Research
759 145, 52–65. https://doi.org/10.1016/j.marenvres.2019.02.004

760 Hurst, T.P., Fernandez, E.R., Mathis, J.T., 2013. Effects of ocean acidification on hatch size and larval
761 growth of walleye pollock (Theragra chalcogramma). ICES Journal of Marine Science 70, 812–822.
762 https://doi.org/10.1093/icesjms/fst053

763 Hurst, T.P., Laurel, Benjamin.J., Ciannelli, L., 2010. Ontogenetic patterns and temperature-dependent
764 growth rates in early life stages of Pacific cod (Gadus macrocephalus). Fishery Bulletin 382–392.

765 Hurst, T.P., Moss, J.H., Miller, J.A., 2012. Distributional patterns of 0-group Pacific cod (Gadus
766 macrocephalus) in the eastern Bering Sea under variable recruitment and thermal conditions. ICES
767 Journal of Marine Science 69, 163–174. https://doi.org/10.1093/icesjms/fss011

768 IPCC, 2021. Climate Change 2021: The Physical Science Basis. Contribution of Working Group I to the
769 Sixth Assessment Report of the Intergovernmental Panel on Climate Change [Masson-Delmotte, V., P.
770 Zhai, A. Pirani, S.L. Connors, C. Péan, S. Berger, N. Caud, Y. Chen, L. Goldfarb, M.I. Gomis, M. Huang, K.
771 Leitzell, E. Lonnoy, J.B.R. Matthews, T.K. Maycock, T. Waterfield, O. Yelekçi, R. Yu, and B. Zhou (eds.)].
772 Cambridge University Press.

773 Kachel, N.B., Hunt, G.L., Salo, S.A., Schumacher, J.D., Stabeno, P.J., Whitledge, T.E., 2002. Characteristics
774 and variability of the inner front of the southeastern Bering Sea. Deep Sea Research Part II: Topical
775 Studies in Oceanography 49, 5889–5909. https://doi.org/10.1016/S0967-0645(02)00324-7

776 Kay, J.E., Deser, C., Phillips, A., Mai, A., Hannay, C., Strand, G., Arblaster, J.M., Bates, S.C., Danabasoglu,
777 G., Edwards, J., Holland, M., Kushner, P., Lamarque, J.-F., Lawrence, D., Lindsay, K., Middleton, A.,
778 Munoz, E., Neale, R., Oleson, K., Polvani, L., Vertenstein, M., 2015. The Community Earth System Model
779 (CESM) Large Ensemble Project: A Community Resource for Studying Climate Change in the Presence of
780 Internal Climate Variability. Bulletin of the American Meteorological Society 96, 1333–1349.
781 https://doi.org/10.1175/BAMS-D-13-00255.1

782 Kearney, K., Hermann, A., Cheng, W., Ortiz, I., Aydin, K., 2020. A coupled pelagic–benthic–sympagic
783 biogeochemical model for the Bering Sea: documentation and validation of the BESTNPZ model
784 (v2019.08.23) within a high-resolution regional ocean model. Geoscientific Model Development 13,
785 597–650. https://doi.org/10.5194/gmd-13-597-2020

786 Kimmel, D.G., Duffy-Anderson, J.T., 2020. Zooplankton abundance trends and patterns in Shelikof Strait,
787 western Gulf of Alaska, USA, 1990–2017. Journal of Plankton Research 42, 334–354.
788 https://doi.org/10.1093/plankt/fbaa019

789 Kleisner, K.M., Fogarty, M.J., McGee, S., Hare, J.A., Moret, S., Perretti, C.T., Saba, V.S., 2017. Marine
790 species distribution shifts on the U.S. Northeast Continental Shelf under continued ocean warming.
791 Progress in Oceanography 153, 24–36. https://doi.org/10.1016/j.pocean.2017.04.001

792 Koenigstein, S., Mark, F.C., Gößling-Reisemann, S., Reuter, H., Poertner, H.-O., 2016. Modelling climate
793 change impacts on marine fish populations: process-based integration of ocean warming, acidification
794 and other environmental drivers. Fish Fish 17, 972–1004. https://doi.org/10.1111/faf.12155

795 Kristiansen, T., Drinkwater, K.F., Lough, R.G., Sundby, S., 2011. Recruitment variability in north Atlantic
796 cod and match-mismatch dynamics. PLoS ONE 6, e17456.
797 https://doi.org/10.1371/journal.pone.0017456

798 Kristiansen, T., Fiksen, Ø., Folkvord, A., 2007. Modelling feeding, growth, and habitat selection in larval
799 Atlantic cod (Gadus morhua): observations and model predictions in a macrocosm environment. Can. J.
800 Fish. Aquat. Sci. 64, 136–151. https://doi.org/10.1139/f06-176

801 Kristiansen, T., Jorgensen, C., Lough, R.G., Vikebo, F., Fiksen, O., 2009. Modeling rule-based behavior:
802 habitat selection and the growth-survival trade-off in larval cod. Behavioral Ecology 20, 490–500.
803 https://doi.org/10.1093/beheco/arp023

804 Kristiansen, T., Stock, C., Drinkwater, K.F., Curchitser, E.N., 2014. Mechanistic insights into the effects of
805 climate change on larval cod. Glob Change Biol 20, 1559–1584. https://doi.org/10.1111/gcb.12489

806 Kroeker, K.J., Kordas, R.L., Crim, R., Hendriks, I.E., Ramajo, L., Singh, G.S., Duarte, C.M., Gattuso, J., 2013.
807 Impacts of ocean acidification on marine organisms: quantifying sensitivities and interaction with
808 warming. Glob Change Biol 19, 1884–1896. https://doi.org/10.1111/gcb.12179

809 Laurel, B.J., Hunsicker, M.E., Ciannelli, L., Hurst, T.P., Duffy-Anderson, J., O'Malley, R., Behrenfeld, M.,
810 2021. Regional warming exacerbates match/mismatch vulnerability for cod larvae in Alaska. Progress in
811 Oceanography 193, 102555. https://doi.org/10.1016/j.pocean.2021.102555

812 Laurel, B.J., Hurst, T.P., Ciannelli, L., 2011. An experimental examination of temperature interactions in
813 the match–mismatch hypothesis for Pacific cod larvae. Can. J. Fish. Aquat. Sci. 68, 51–61.
814 https://doi.org/10.1139/F10-130

815 Laurel, B.J., Hurst, T.P., Copeman, L.A., Davis, M.W., 2008. The role of temperature on the growth and
816 survival of early and late hatching Pacific cod larvae (Gadus macrocephalus). Journal of Plankton
817 Research 30, 1051–1060. https://doi.org/10.1093/plankt/fbn057

818 Laurel, B.J., Rogers, L.A., 2020. Loss of spawning habitat and prerecruits of Pacific cod during a Gulf of
819 Alaska heatwave. Can. J. Fish. Aquat. Sci. 77, 644–650. https://doi.org/10.1139/cjfas-2019-0238

820 Lewis, C.N., Brown, K.A., Edwards, L.A., Cooper, G., Findlay, H.S., 2013. Sensitivity to ocean acidification
821 parallels natural pCO2 gradients experienced by Arctic copepods under winter sea ice. Proceedings of
822 the National Academy of Sciences 110, E4960–E4967. https://doi.org/10.1073/pnas.1315162110

MacKenzie, B.R., Kiørboe, T., 1995. Encounter rates and swimming behavior of pause-travel and cruise larval fish predators in calm and turbulent laboratory environments. Limnol. Oceanogr. 40, 1278–1289. https://doi.org/10.4319/lo.1995.40.7.1278

Maneja, R., Frommel, A., Geffen, A., Folkvord, A., Piatkowski, U., Chang, M., Clemmesen, C., 2013. Effects of ocean acidification on the calcification of otoliths of larval Atlantic cod Gadus morhua. Mar. Ecol. Prog. Ser. 477, 251–258. https://doi.org/10.3354/meps10146

Mathis, J., Cross, J., Evans, W., Doney, S., 2015. Ocean Acidification in the Surface Waters of the Pacific-Arctic Boundary Regions. oceanog 25, 122–135. https://doi.org/10.5670/oceanog.2015.36

McLaskey, A., Keister, J., McElhany, P., Brady Olson, M., Shallin Busch, D., Maher, M., Winans, A., 2016. Development of Euphausia pacifica (krill) larvae is impaired under pCO2 levels currently observed in the Northeast Pacific. Mar. Ecol. Prog. Ser. 555, 65–78. https://doi.org/10.3354/meps11839

McLaskey, A.K., Keister, J.E., Schoo, K.L., Olson, M.B., Love, B.A., 2019. Direct and indirect effects of elevated CO2 are revealed through shifts in phytoplankton, copepod development, and fatty acid accumulation. PLoS ONE 14, e0213931. https://doi.org/10.1371/journal.pone.0213931

Meinshausen, M., Smith, S.J., Calvin, K., Daniel, J.S., Kainuma, M.L.T., Lamarque, J.-F., Matsumoto, K., Montzka, S.A., Raper, S.C.B., Riahi, K., Thomson, A., Velders, G.J.M., van Vuuren, D.P.P., 2011. The RCP greenhouse gas concentrations and their extensions from 1765 to 2300. Climatic Change 109, 213–241. https://doi.org/10.1007/s10584-011-0156-z

Moss, R.H., Edmonds, J.A., Hibbard, K.A., Manning, M.R., Rose, S.K., van Vuuren, D.P., Carter, T.R., Emori, S., Kainuma, M., Kram, T., Meehl, G.A., Mitchell, J.F.B., Nakicenovic, N., Riahi, K., Smith, S.J., Stouffer, R.J., Thomson, A.M., Weyant, J.P., Wilbanks, T.J., 2010. The next generation of scenarios for climate change research and assessment. Nature 463, 747–756. https://doi.org/10.1038/nature08823

Mueter, F.J., Bond, N.A., Ianelli, J.N., Hollowed, A.B., 2011. Expected declines in recruitment of walleye pollock (Theragra chalcogramma) in the eastern Bering Sea under future climate change. ICES Journal of Marine Science 68, 1284–1296. https://doi.org/10.1093/icesjms/fsr022

Mueter, F.J., Litzow, M.A., 2008. Sea ice retreat alters biogeography of the Bering sea continental shelf. Ecological Applications 18, 309–320. https://doi.org/10.1890/07-0564.1

Munday, P.L., Leis, J.M., Lough, J.M., Paris, C.B., Kingsford, M.J., Berumen, M.L., Lambrechts, J., 2009. Climate change and coral reef connectivity. Coral Reefs 17.

Nagelkerken, I., Munday, P.L., 2016. Animal behaviour shapes the ecological effects of ocean acidification and warming: moving from individual to community-level responses. Glob Change Biol 22, 974–989. https://doi.org/10.1111/gcb.13167

Nagelkerken, I., Russell, B.D., Gillanders, B.M., Connell, S.D., 2016. Ocean acidification alters fish populations indirectly through habitat modification. Nature Clim Change 6, 89–93. https://doi.org/10.1038/nclimate2757

Neidetcher, S.K., Hurst, T.P., Ciannelli, L., Logerwell, E.A., 2014. Spawning phenology and geography of Aleutian Islands and eastern Bering Sea Pacific cod (Gadus macrocephalus). Deep Sea Research Part II: Topical Studies in Oceanography 109, 204–214. https://doi.org/10.1016/j.dsr2.2013.12.006

Ottersen, G., Kim, S., Huse, G., Polovina, J.J., Stenseth, N.Chr., 2010. Major pathways by which climate may force marine fish populations. Journal of Marine Systems 79, 343–360. https://doi.org/10.1016/j.jmarsys.2008.12.013

Peck, M.A., Hufnagl, M., 2012. Can IBMs tell us why most larvae die in the sea? Model sensitivities and scenarios reveal research needs. Journal of Marine Systems 93, 77–93. https://doi.org/10.1016/j.jmarsys.2011.08.005

Pilcher, D.J., Cross, J.N., Hermann, A.J., Kearney, K.A., Cheng, W., Mathis, J.T., 2022. Dynamically downscaled projections of ocean acidification for the Bering Sea. Deep Sea Research Part II: Topical Studies in Oceanography 198, 105055. https://doi.org/10.1016/j.dsr2.2022.105055

Pilcher, D.J., Naiman, D.M., Cross, J.N., Hermann, A.J., Siedlecki, S.A., Gibson, G.A., Mathis, J.T., 2019. Modeled Effect of Coastal Biogeochemical Processes, Climate Variability, and Ocean Acidification on Aragonite Saturation State in the Bering Sea. Front. Mar. Sci. 5, 508. https://doi.org/10.3389/fmars.2018.00508

Pinsky, M.L., Worm, B., Fogarty, M.J., Sarmiento, J.L., Levin, S.A., 2013. Marine Taxa Track Local Climate Velocities. Science 341, 1239–1242. https://doi.org/10.1126/science.1239352

Punt, A.E., Foy, R.J., Dalton, M.G., Long, W.C., Swiney, K.M., 2016. Effects of long-term exposure to ocean acidification conditions on future southern Tanner crab (Chionoecetes bairdi) fisheries management. ICES Journal of Marine Science 73, 849–864. https://doi.org/10.1093/icesjms/fsv205

R Core Team, 2022. R: A Language and Environment for Statistical Computing. R Foundation for Statistical Computing, Vienna, Austria.

Rooper, C.N., Ortiz, I., Hermann, A.J., Laman, N., Cheng, W., Kearney, K., Aydin, K., 2021. Predicted shifts of groundfish distribution in the Eastern Bering Sea under climate change, with implications for fish populations and fisheries management. ICES Journal of Marine Science 78, 220–234. https://doi.org/10.1093/icesjms/fsaa215

Shchepetkin, A.F., McWilliams, J.C., 2005. The regional oceanic modeling system (ROMS): a split-explicit, free-surface, topography-following-coordinate oceanic model. Ocean Modelling 9, 347–404. https://doi.org/10.1016/j.ocemod.2004.08.002

Spies, I., Gruenthal, K.M., Drinan, D.P., Hollowed, A.B., Stevenson, D.E., Tarpey, C.M., Hauser, L., 2020. Genetic evidence of a northward range expansion in the eastern Bering Sea stock of Pacific cod. Evol Appl 13, 362–375. https://doi.org/10.1111/eva.12874

Stabeno, P.J., Bond, N.A., Kachel, N.B., Salo, S.A., Schumacher, J.D., 2001. On the temporal variability of the physical environment over the south-eastern Bering Sea. Fisheries Oceanography 10, 81–98. https://doi.org/10.1046/j.1365-2419.2001.00157.x

Stabeno, P.J., Danielson, S.L., Kachel, D.G., Kachel, N.B., Mordy, C.W., 2016. Currents and transport on the Eastern Bering Sea shelf: An integration of over 20 years of data. Deep Sea Research Part II: Topical Studies in Oceanography 134, 13–29. https://doi.org/10.1016/j.dsr2.2016.05.010

Stabeno, P.J., Duffy-Anderson, J.T., Eisner, L.B., Farley, E.V., Heintz, R.A., Mordy, C.W., 2017. Return of warm conditions in the southeastern Bering Sea: Physics to fluorescence. PLoS ONE 12, e0185464. https://doi.org/10.1371/journal.pone.0185464

Stevenson, D.E., Lauth, R.R., 2019. Bottom trawl surveys in the northern Bering Sea indicate recent shifts in the distribution of marine species. Polar Biol 42, 407–421. https://doi.org/10.1007/s00300-018-2431-1

Stiasny, M.H., Mittermayer, F.H., Sswat, M., Voss, R., Jutfelt, F., Chierici, M., Puvanendran, V., Mortensen, A., Reusch, T.B.H., Clemmesen, C., 2016. Ocean Acidification Effects on Atlantic Cod Larval Survival and Recruitment to the Fished Population. PLoS ONE 11, e0155448. https://doi.org/10.1371/journal.pone.0155448

Stiasny, M.H., Sswat, M., Mittermayer, F.H., Falk-Petersen, I., Schnell, N.K., Puvanendran, V., Mortensen, A., Reusch, T.B.H., Clemmesen, C., 2019. Divergent responses of Atlantic cod to ocean acidification and food limitation. Glob Change Biol 25, 839–849. https://doi.org/10.1111/gcb.14554

Stockhausen, W.T., Coyle, K.O., Hermann, A.J., Blood, D., Doyle, M.J., Gibson, G.A., Hinckley, S., Ladd, C., Parada, C., 2019a. Running the gauntlet: Connectivity between spawning and nursery areas for arrowtooth flounder (Atheresthes stomias) in the Gulf of Alaska, as inferred from a biophysical individual-based model. Deep Sea Research Part II: Topical Studies in Oceanography 165, 127–139. https://doi.org/10.1016/j.dsr2.2018.05.017

Stockhausen, W.T., Coyle, K.O., Hermann, A.J., Doyle, M., Gibson, G.A., Hinckley, S., Ladd, C., Parada, C., 2019b. Running the gauntlet: Connectivity between natal and nursery areas for Pacific ocean perch (Sebastes alutus) in the Gulf of Alaska, as inferred from a biophysical individual-based model. Deep Sea Research Part II: Topical Studies in Oceanography 165, 74–88. https://doi.org/10.1016/j.dsr2.2018.05.016

Szuwalski, C., Cheng, W., Foy, R., Hermann, A.J., Hollowed, A., Holsman, K., Lee, J., Stockhausen, W., Zheng, J., 2021. Climate change and the future productivity and distribution of crab in the Bering Sea. ICES Journal of Marine Science 78, 502–515. https://doi.org/10.1093/icesjms/fsaa140

Taylor, K.E., Stouffer, R.J., Meehl, G.A., 2012. An Overview of CMIP5 and the Experiment Design. Bulletin of the American Meteorological Society 93, 485–498. https://doi.org/10.1175/BAMS-D-11-00094.1

Vehmaa, A., Almén, A.-K., Brutemark, A., Paul, A., Riebesell, U., Furuhagen, S., Engström-Öst, J., 2016. Ocean acidification challenges copepod phenotypic plasticity. Biogeosciences 13, 6171–6182. https://doi.org/10.5194/bg-13-6171-2016

Wang, M., Jeong, C.-B., Lee, Y.H., Lee, J.-S., 2018. Effects of ocean acidification on copepods. Aquatic Toxicology 196, 17–24. https://doi.org/10.1016/j.aquatox.2018.01.004

Watanabe, S., Hajima, T., Sudo, K., Nagashima, T., Takemura, T., Okajima, H., Nozawa, T., Kawase, H., Abe, M., Yokohata, T., Ise, T., Sato, H., Kato, E., Takata, K., Emori, S., Kawamiya, M., 2011. MIROC-ESM 2010: model description and basic results of CMIP5-20c3m experiments. Geosci. Model Dev. 4, 845–872. https://doi.org/10.5194/gmd-4-845-2011

West, C.F., Etnier, M.A., Barbeaux, S., Partlow, M.A., Orlov, A.M., 2020. Size distribution of Pacific cod (Gadus macrocephalus) in the North Pacific Ocean over 6 millennia. Quat. res. 1–21. https://doi.org/10.1017/qua.2020.70

Whitehouse, G.A., Aydin, K., Hollowed, A., Holsman, K., Cheng, W., Faig, A., Haynie, A.C., Hermann, A., Kearney, K., Punt, A.E., Essington, T.E., 2021. Bottom–Up Impacts of Forecasted Climate Change on the Eastern Bering Sea Food Web. Frontiers in Marine Science 8, 20. https://doi.org/10.3389/fmars.2021.624301

Woolley, L.D., Qin, J.G., 2010. Swimbladder inflation and its implication to the culture of marine finfish larvae: Swimbladder inflation in fish larvae. Reviews in Aquaculture 2, 181–190. https://doi.org/10.1111/j.1753-5131.2010.01035.x

945

Tables

Table 1. Variables and parameters in the individual-based model (IBM).

Symbol	Description	Units	Value
Parameters			
C_0	Inherent contrast (visibility) of the prey	–	0.3
K_e	Satiation parameter	$\mu E.m^{-2}.s^{-1}$	1
f	Pause frequency	s^{-1}	0.43
λ	Pause duration	s	2
l_{max}	Maximum prey length that a fish can capture relative to fish length	–	0.1
m_s	Mortality constant (only when stomach was empty)	s^{-1}	1.10^{-5}
K_p	Constant in visual predation (comprising all other factors such as predator density, efficiency, and predator swimming speed)	–	7.10^{-6}
Variables			
A_p	Prey area	mm^{-2}	
E_b	Local illumination level	$\mu mol.m^{-2}.s^{-1}$	
E'	Size-specific sensitivity of the visual system of the larvae	–	
c	Beam attenuation coefficient	mm^{-1}	
N	Prey density	$prey.mm^{-3}$	
u	Prey swimming velocity	$mm.s^{-1}$	
ω	Turbulent velocity	$mm.s^{-1}$	
T	Temperature	℃	
t	Time step index	–	

L	Fish standard length	mm	
TL	Fish total length	mm	
dt	Model time-step length	$days$	
l	Prey length	mm	
w_{prey}	Prey weight	mg	
i	Index over prey lengths	$-$	
j	Index over prey types	$-$	
k	Index over particles	$-$	
z	Index over initial locations	$-$	

10

11 Table 2. Main equations in the individual-based model (IBM).

Symbol	Description	Equation	Units	Equation number	Source
Egg stage					
g_{Ew}	Growth rate in weight	$3.807 + 1.493.T - 0.032.T^2$	$\frac{1}{d}$	1	(Hurst et al., 2010)
g_{El}	Growth rate in length	$0.104 + 0.024.T - 0.00002.T^2$	$mm.d^{-1}$	2	(Hurst et al., 2010)
d_E	Stage duration	$46.597 - 4.079.T$	d	3	(Hinckley et al., 2019)
h_E	Hatching success	$\frac{0.453}{1 + ((T - 4.192)/2.125)^2}$	$-$	4	(Laurel and Rogers, 2020)
Yolk-sac stage					
YSA	Days to yolk-sac absorption	$14.7662.exp\,(-0.235.T)$	d	5	(Laurel et al., 2008)
PNR	Point of no-return	$34.67.exp\,(-0.126.T)$	d	6	(Laurel et al., 2008)
Non-egg stages					
g	Growth rate in weight	$(0.454 + 1.61.T - 0.069.T^2 \; exp\,(-2.225.w))$	$\frac{1}{d}$	7	(Hurst et al., 2010)

L	Fish standard length	$\left(\frac{w}{1.976.10^{-6}}\right)^{\frac{1}{2.974}}$	mm	8	Estimates from Hurst et al. (2010)
TL	Fish total length	$\frac{L+0.5169}{0.9315}$	mm	9	Estimates from Hurst et al. (2010)
ϑ_F	Vertical velocity	$\frac{(0.081221+0.043168.log_{10}T).TL^{1.49652}}{1000}$	$m.s^{-1}$	10	(Hinckley et al., 2019)
Bioenergetic model					
R	Reactive distance	$R^2 exp\,(cR) = C_0 A_p E' \frac{E_b}{K_e+E_b}$	mm	11	(Fiksen and MacKenzie, 2002)
enc	Encounter rate	$\frac{2}{3}\pi R^3 Nf + \pi R^2 N\sqrt{(u^2+2\omega^2)}f\lambda$	$prey.s^{-1}$	12	(Fiksen and MacKenzie, 2002)
$PCA\,(L \leq 17\,mm)$	Probability of attack success	Algorithm in Fiksen and MacKenzie (2002)	–	13	(Fiksen and MacKenzie, 2002)
$PCA\,(L > 17\,mm)$	Probability of attack success	$1.1-(\frac{1.1.l}{l_{max}})$	–	14	(Daewel et al., 2011)
h	Handling time	$exp(0.264.10^{7.0151.(\frac{l}{L})})$	s	15	(Walton et al., 1992)
ing	Ingested prey	$\frac{\sum_{i,j} enc_{i,j}.PCA_{i,j}.w_{prey_{i,j}}}{1+\sum_{i,j} enc_{i,j}.h_{i,j}}$	mg	16	(Daewel et al., 2011)
A	Assimilation efficiency	$0.8.(1-0.4.exp(-0.002.(w.1000-50)))$	–	17	(Lough et al., 2005)

D_{max}	Ingested material required for maximum growth	$\frac{((exp\,(g.dt)\ -1).w_{t-1} + M_a.dt)}{A}$	mg	18	(Kristiansen et al., 2014)
S_t	Stomach content	$S_{t-1} - D + ing$	mg	19	(Kristiansen et al., 2014)
M_r	Routine metabolism	$2.38e^{-7}w^{0.9}exp(0.088.T)$	$mg.d^{-1}$	20	(Finn et al., 2002)
M_a	Active metabolism (when $E_b > 0.001$)	$\begin{cases} 2.5M_r & if\ L \geq 5.5\ mm \\ 1.4M_r & if\ L < 5.5\ mm \end{cases}$	$mg.d^{-1}$	21	(Finn et al., 2002)
w_t	Fish dry weight	$\begin{cases} w_{t-1}.exp\,(g.dt) & if\ D_{max} \leq S_t \\ w_{t-1} + S_tA - M_a.dt & if\ D_{max} > S_t \end{cases}$	mg	22	(Kristiansen et al., 2014)

Figures

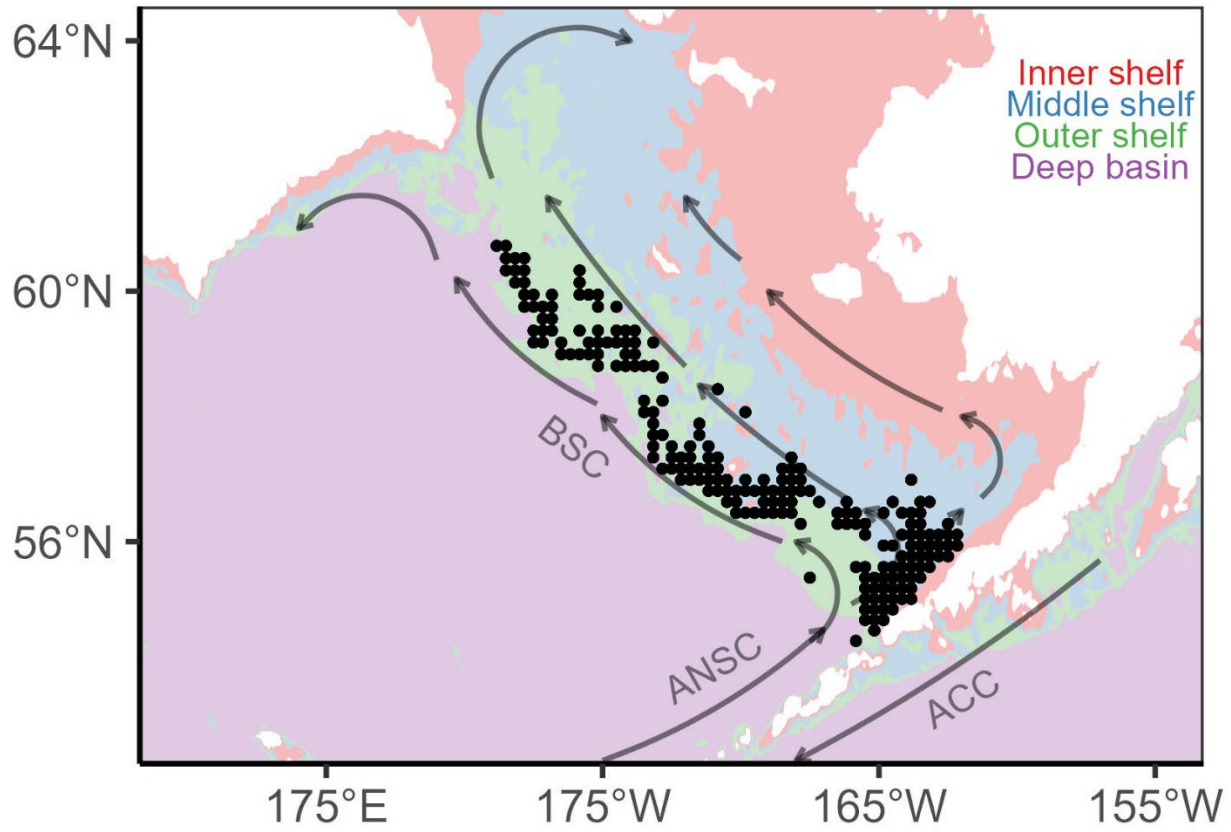

Figure 1. Study region (Bering Sea) with bathymetry (m) domains (colors). Red = inner shelf domain (0-50 m), blue = middle shelf domain (50-100 m), green = outer shelf domain (100-200 m), purple = deep basin (>200 m). Main oceanic currects are shown (arrows) as described in Stabeno et al. (2016). ANSC = Aleutian North Slope, BSC = Bering Slope Current, ACC = Alaska Coastal Current. Black dots represent the locations where eggs were released every seven days during March every year in the IBM.

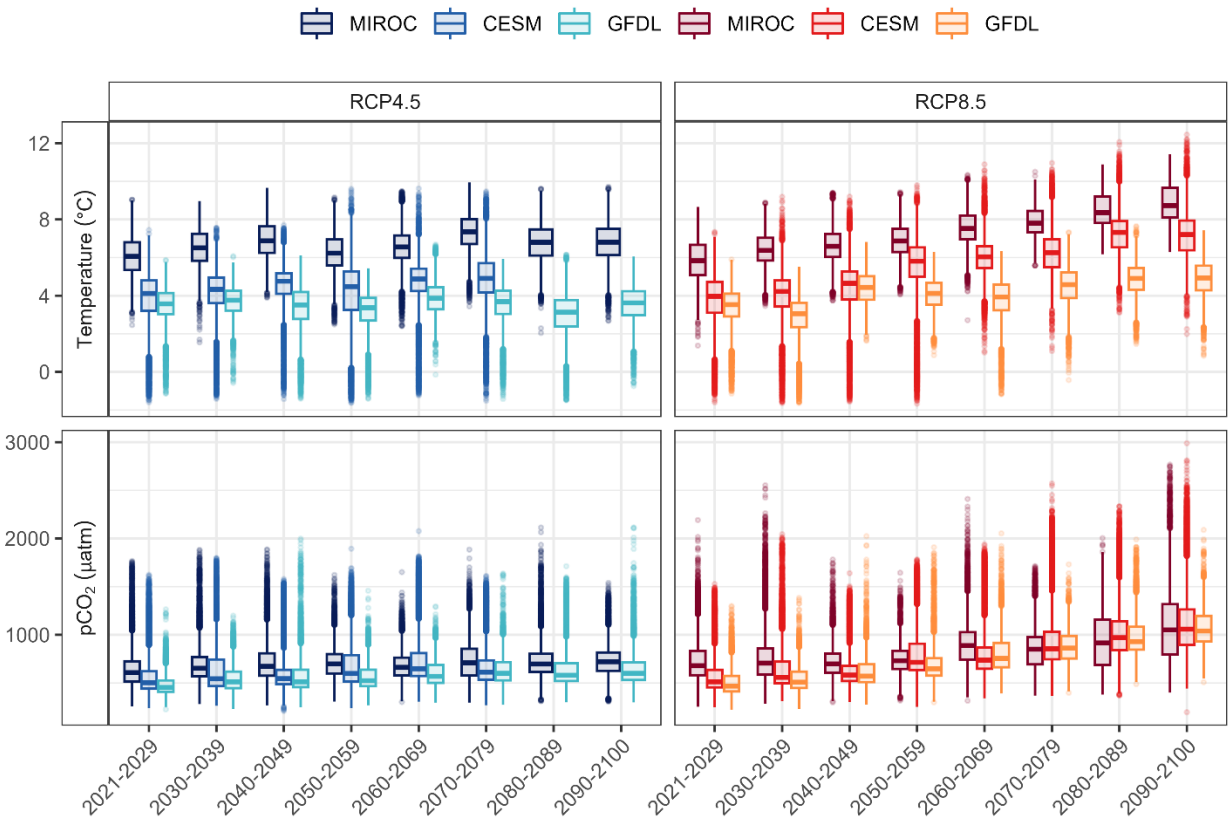

Figure 2. Average environmental conditions experienced by fish (surviving and dead) throughout the non-egg stages each decade. Values are shown for the RCP4.5 (blue tones) and RCP8.5 (red tones) emission scenarios and oceanographic models.

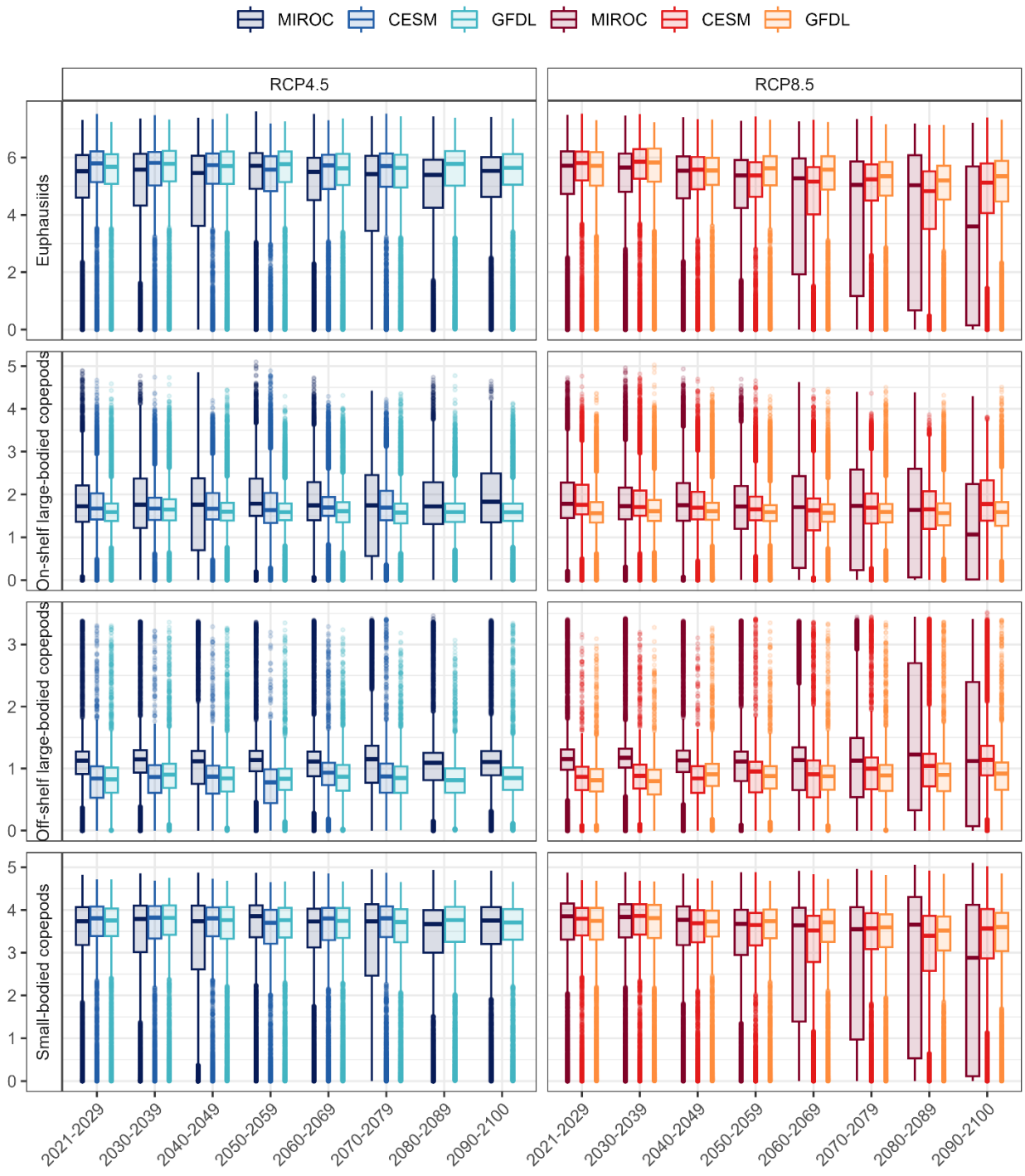

Figure 3. Average prey density (mg C/m^3) in the environment where fish (surviving and dead) dwelled through the non-egg stages. Values are shown for the RCP4.5 (blue tones) and RCP8.5 (red tones) emission scenarios and oceanographic model by decade.

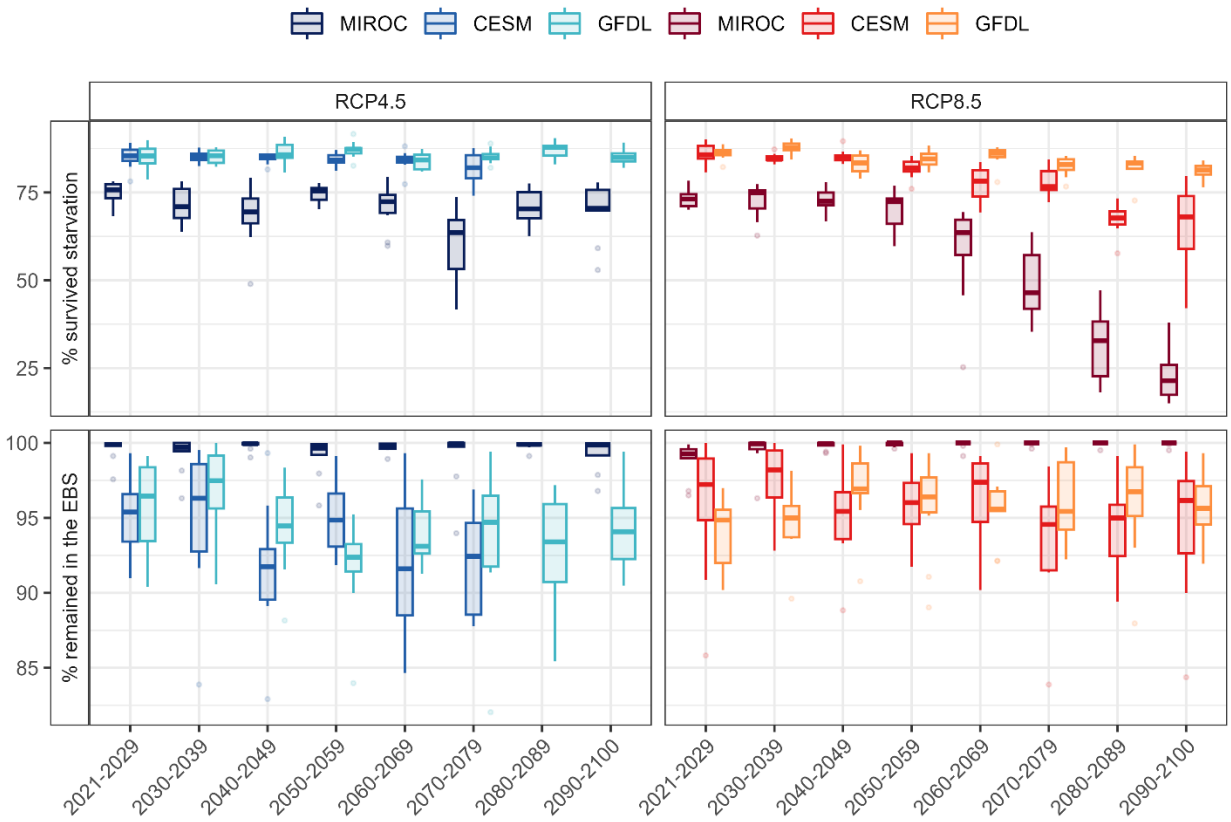

Figure 4. Percentage of fish that survived until Sep 15, separated by death cause. Values are shown for the RCP4.5 (blue tones) and RCP8.5 (red tones) emission scenarios and oceanographic model by decade.

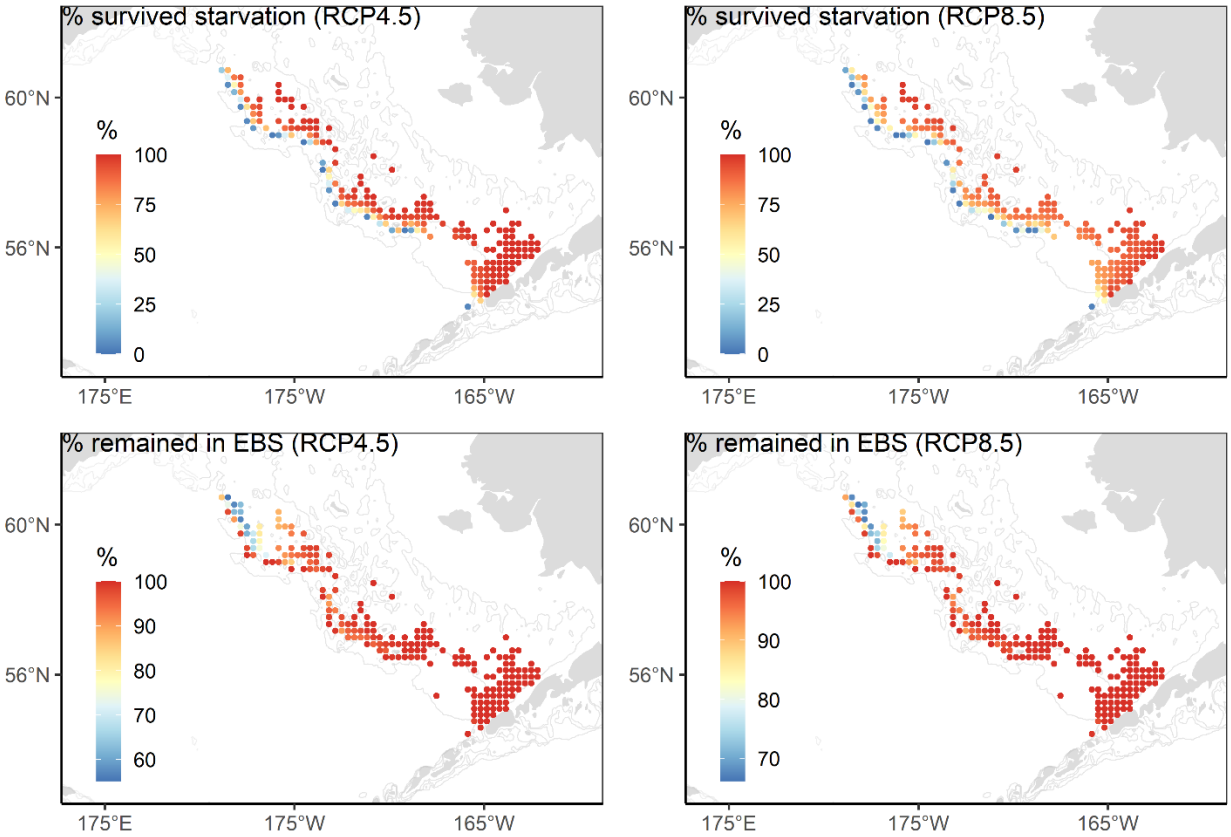

Figure 5. Percentage of fish that survived to Sep 15, separated by death cause, over the years and displayed by release location. Oceanographic models were combined. Values are shown for the RCP4.5 (left column) and RCP8.5 (right column) emission scenarios.

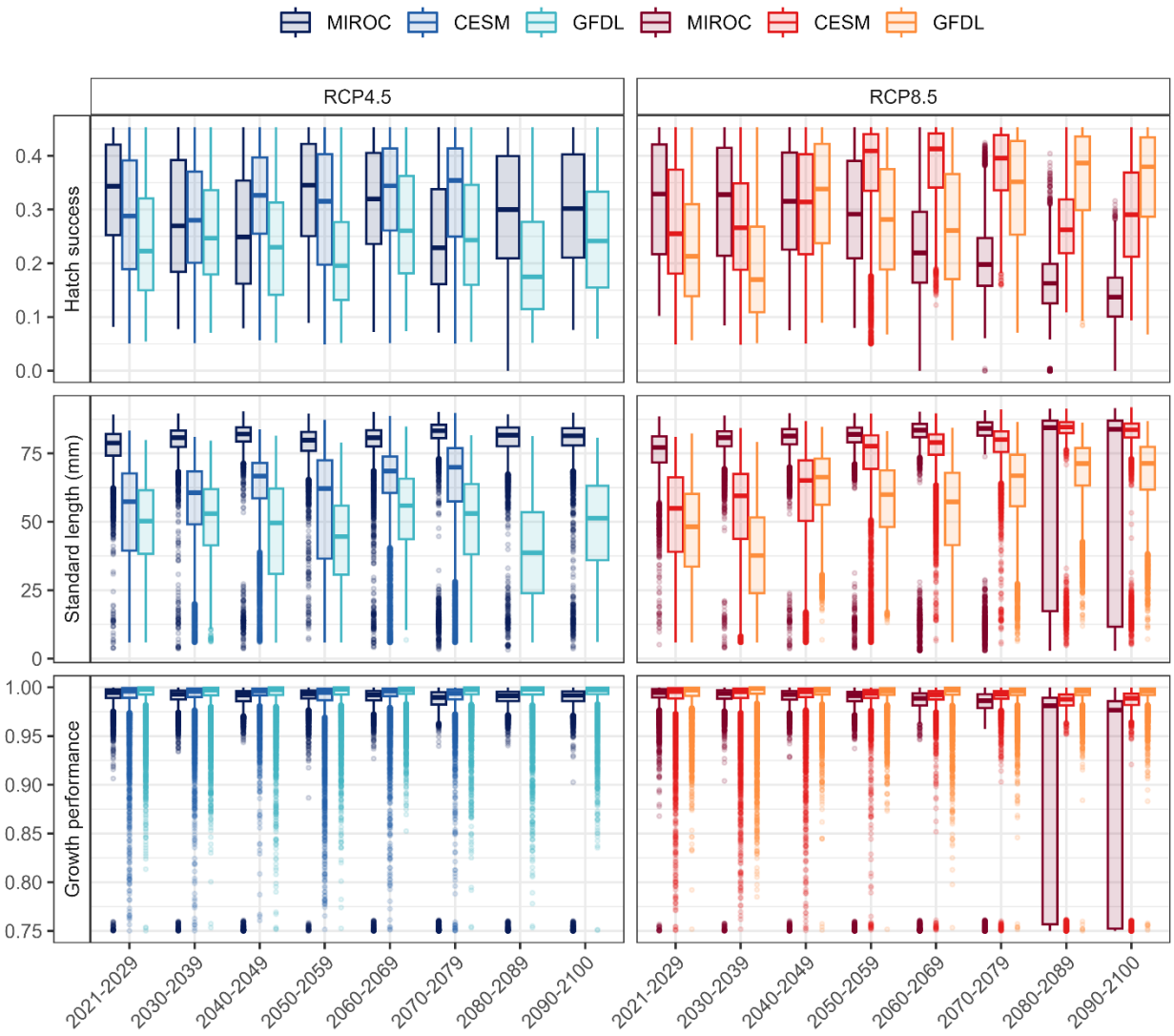

Figure 6. Biological variables for fish that survived until Sep 15. The standard length is calculated on Sep 15. Growth performance is the average value after yolk-sac absorption (YSA). Values are shown for the RCP4.5 (blue tones) and RCP8.5 (red tones) emission scenarios and oceanographic model by decade.

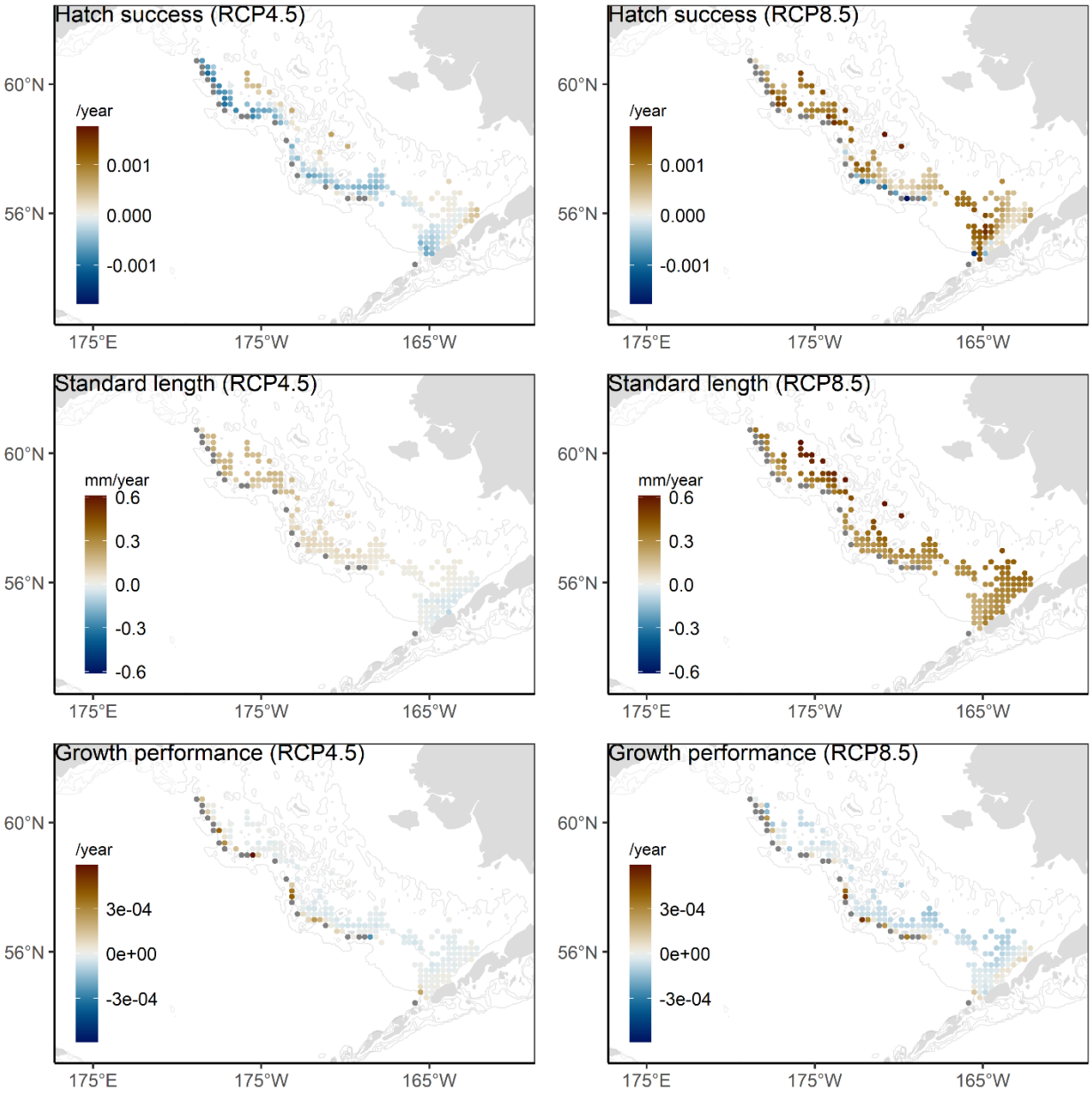

Figure 7. Temporal trends of biological variables displayed by release location. Values are shown for the RCP4.5 (left column) and RCP8.5 (right column) emission scenarios. Information from different oceanographic models was combined to estimate the temporal trend. Temporal trends were not calculated for fish that died more than 33% of the years (grey points).

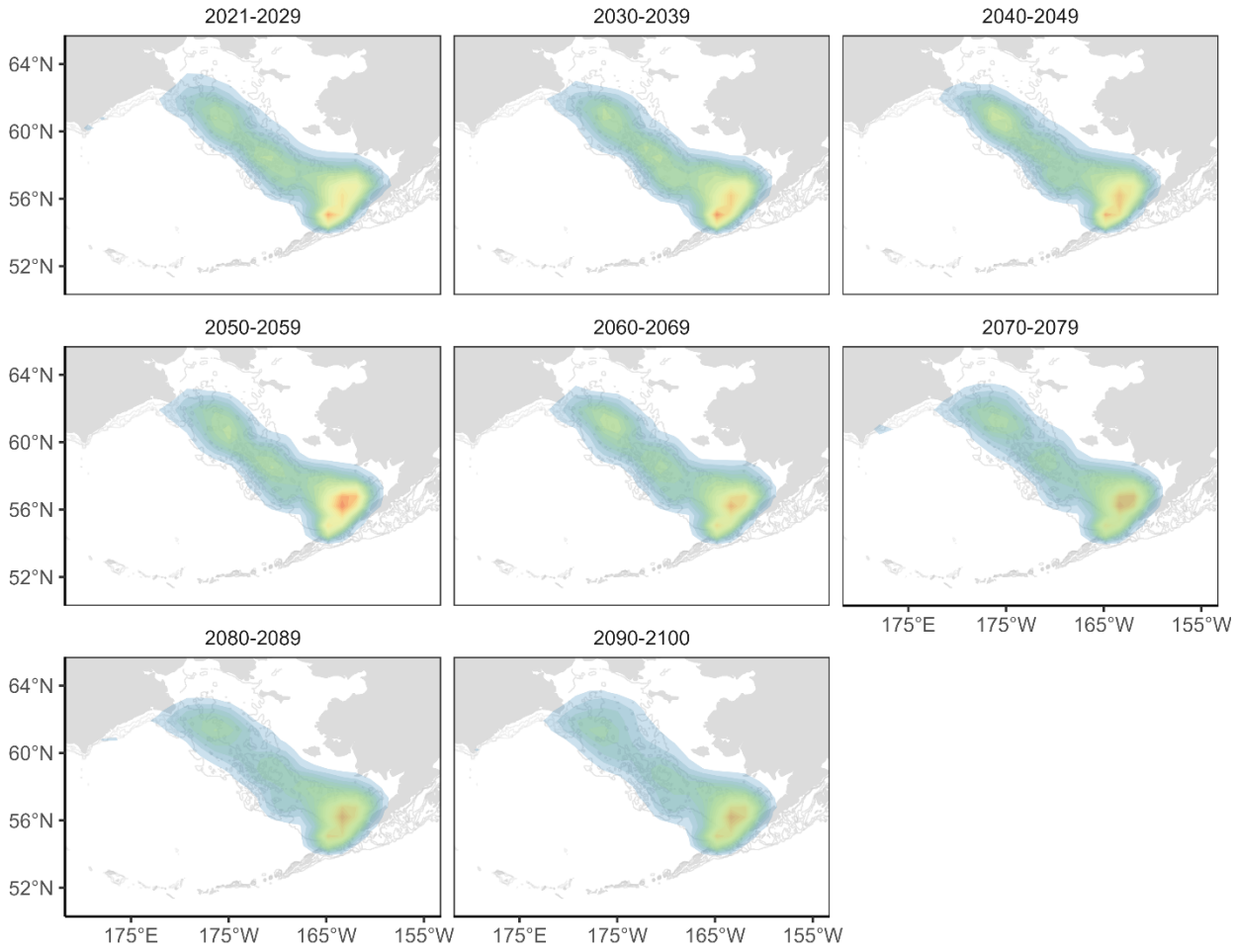

Figure 8. Spatial density of final locations (Sep 15) by decade for the RCP8.5 emission scenario. Information from different oceanographic models was combined. Red and blue colors indicate higher and lower densities, respectively.

a) Current conditions

b) Future conditions (RCP8.5)

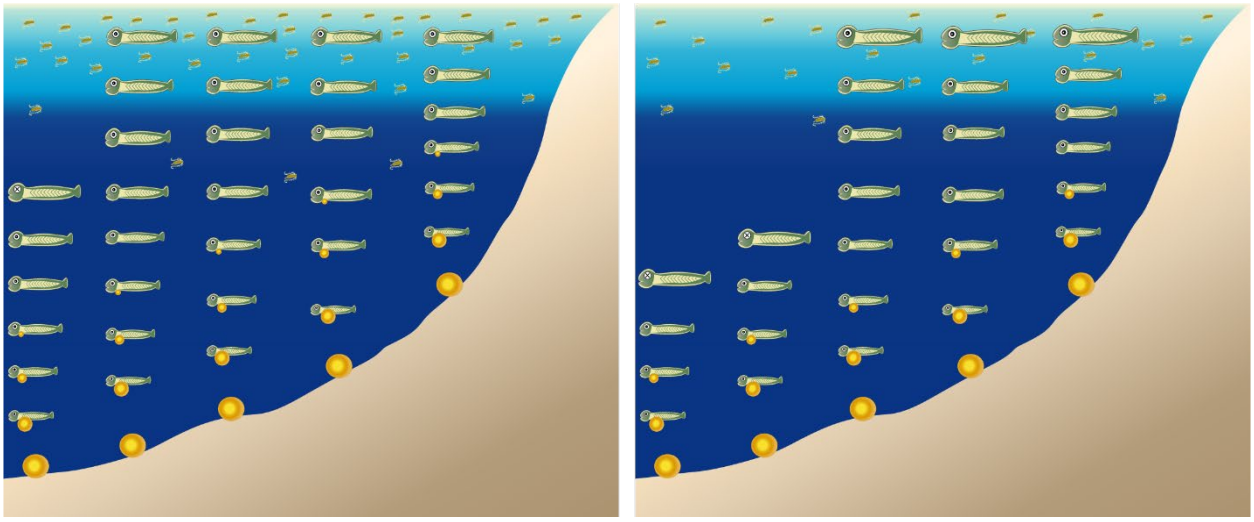

Figure 9. Representation of the impacts of climate on larval ecology during current and future conditions (RCP8.5). We represent the transition from eggs to the epipelagic juvenile stage for five fish vertically. In current conditions, prey density is high, especially in the epipelagic zone (sky-blue area). Fish that hatched from eggs in deeper locations have a higher probability of starvation since more time is spent in areas with no light (dark blue area) after yolk-sac absorption; therefore, food ingestion is limited. In future conditions (RCP8.5), prey density is predicted to decrease, and a warmer temperature produces a quicker yolk-sac absorption; therefore, more fish are susceptible to starvation, especially those hatched in deeper areas.

Supplementary information

Tables

Table S1. Prey items obtained from the Bering 10K model (bulk carbon biomass in $mg\ C.m^{-3}$). Size range (mm) and parameters of the length-weight relationship ($w_{prey} = al^b$, w_{prey} is weight in μg and l is the total length in μm) are given per prey item.

Description	**Size range (mm)**	**Parameters**	**Source**
Euphausiids (primarily *Thysanoessa inermis* and *Thysanoessa raschii*)	3-30	a = 1.38E-8, b = 2.92	(Becker and Warren, 2014; Harding, 1977; Saunders et al., 2013; Silva et al., 2017)
On-shelf large-bodied copepods (primarily *Calanus marshallae*)	0.4-3	a = 2.75E-12, b = 4.03	(Liu and Hopcroft, 2007)
Off-shelf large-bodied copepods (primarily *Neocalanus* sp.)	0.2-1.4	a = 1E-10, b = 3.56	(Liu and Hopcroft, 2006)
Small-bodied copepods (e.g. *Pseudocalanus* sp.)	0.2-1.4	a = 2.4E-8, b = 2.85	(Liu and Hopcroft, 2008)

Table S2. Model runs performed. For the ocean acidification (OA) impacts, we assumed effects on five biological components individually, all of them simultaneously, or none of them. The period for which the OA effects were evaluated is also shown.

Earth system model	CO_2 emission scenario	Ocean acidification impact
Geophysical Fluid Dynamics Laboratory Earth System Model 2M (GFDL)	- RCP4.5 - RCP8.5	- All (2021-2100) - Metabolism (2090-2100) - Growth (2090-2100) - Probability of capture success (2090-2100) - Prey abundance (2090-2100) - Prey quality (2090-2100) - None (2090-2100)
National Center for Atmospheric Research Community Earth System Model (CESM)	- RCP4.5 - RCP8.5	- All (2021-2100) - Metabolism (2090-2100) - Growth (2090-2100) - Probability of capture success (2090-2100) - Prey abundance (2090-2100) - Prey quality (2090-2100) - None (2090-2100)
Model for Interdisciplinary Research on Climate (MIROC)	- RCP4.5 - RCP8.5	- All (2021-2100) - Metabolism (2090-2100) - Growth (2090-2100) - Probability of capture success (2090-2100) - Prey abundance (2090-2100) - Prey quality (2090-2100) - None (2090-2100)

Figures

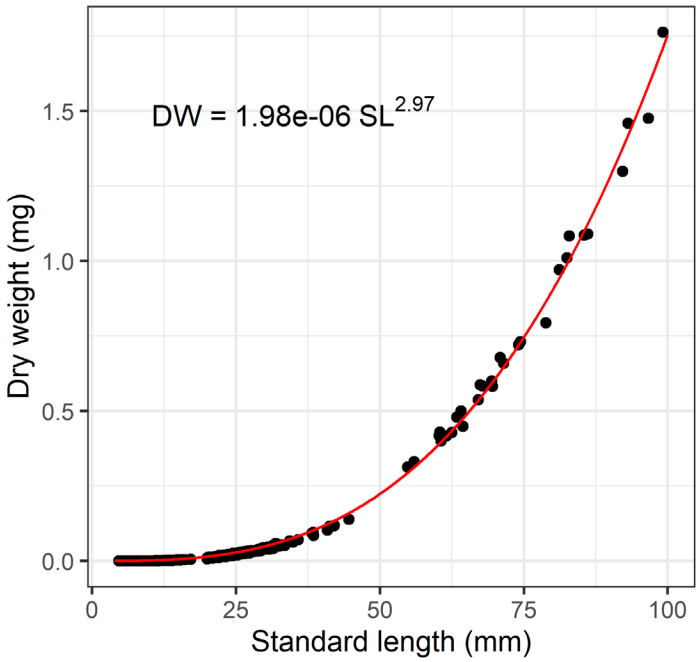

Figure S1. Observed standard length-dry weight relationship and fitted curve to predict fish standard length (L) based on dry weight (w).

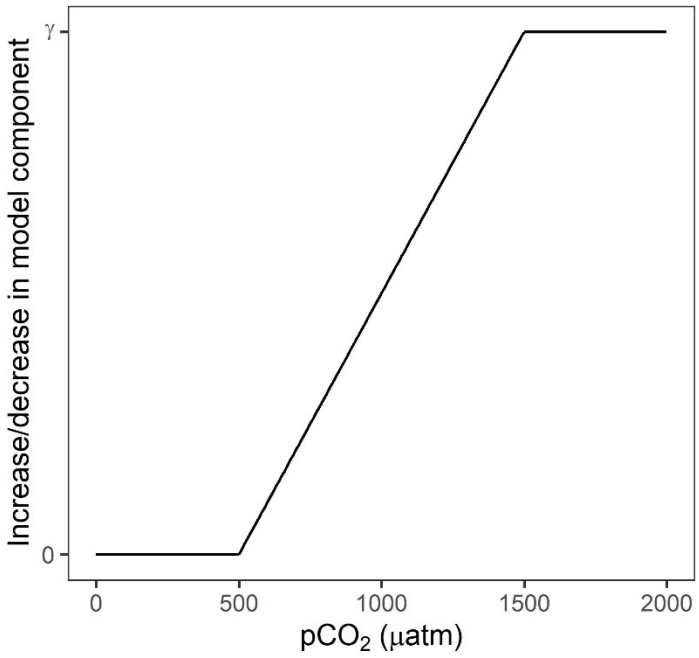

Figure S2. Impacts of a range of pCO_2 values on selected model variables in our model. $\gamma = -10\%$ for active metabolism. $\gamma = -10\%$ for growth rates within the first two weeks after hatching and then +10% within the next five weeks. $\gamma = -10\%$ for prey abundance. $\gamma = -10\%$ for prey weight. $\gamma = -10\%$ for the probability of capture success (PCA).

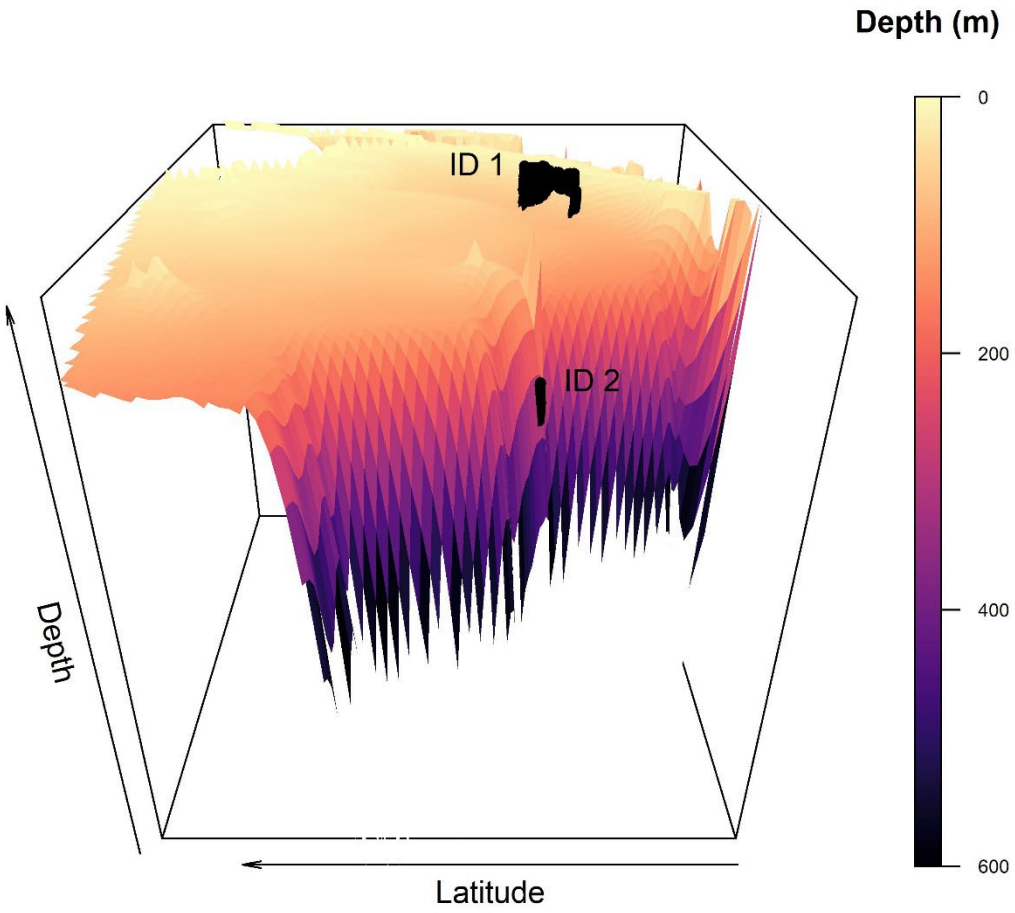

Figure S3. Trajectories of two particles (i.e., fish) in the IBM. The coloured area represents the ocean bottom. The black dots represent the fish location in every model time step. ID 1 was released on a shallower area and survived until the end of the model period (Sep 15th). ID 2 was released in a deeper area and died from starvation (reaching the PNR). Average environmental conditions in the fish habitat were calculated during the fish lifespan.

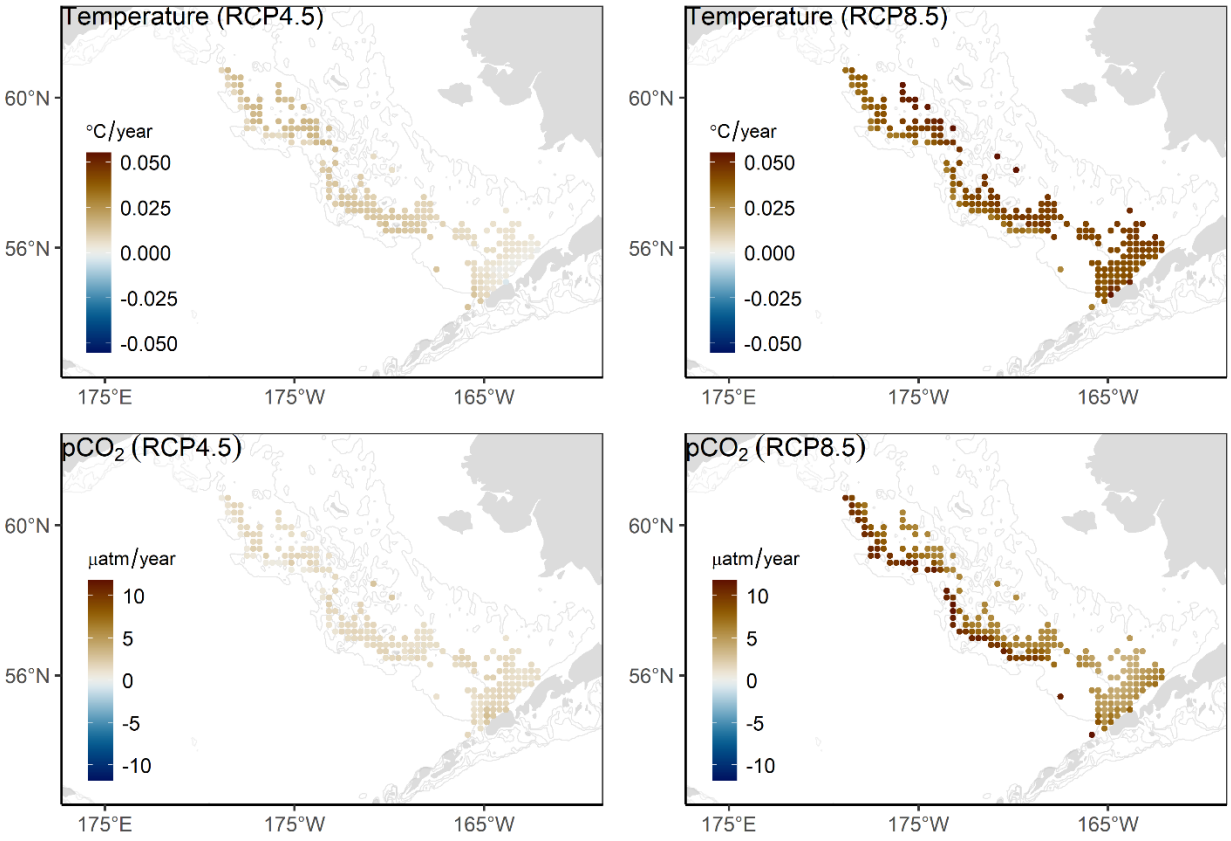

Figure S4. Temporal trends of average environmental conditions where fish (surviving and dead) dwelled throughout the non-egg stages displayed by release location. Values are shown for the RCP4.5 (left column) and RCP8.5 (right column) emission scenarios. Information from different oceanographic models was combined to estimate temporal trends.

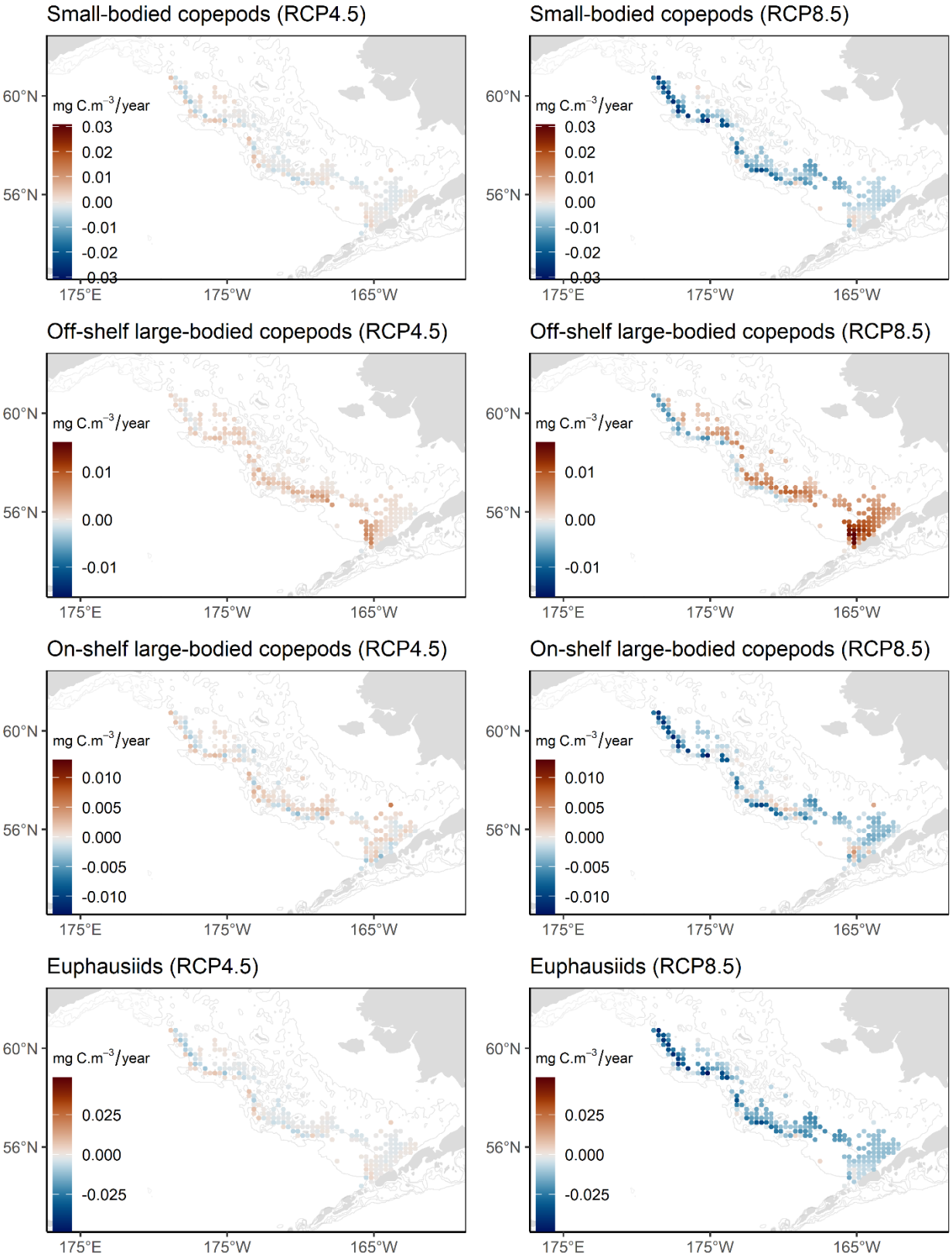
Small-bodied copepods (RCP4.5)
Small-bodied copepods (RCP8.5)
Off-shelf large-bodied copepods (RCP4.5)
Off-shelf large-bodied copepods (RCP8.5)
On-shelf large-bodied copepods (RCP4.5)
On-shelf large-bodied copepods (RCP8.5)
Euphausiids (RCP4.5)
Euphausiids (RCP8.5)
mg C.m^{-3}/year
60°N
56°N
175°E
175°W
165°W
0.03
0.02
0.01
0.00
-0.01
-0.02
-0.03
0.010
0.005
0.000
-0.005
-0.010
0.025
0.000
-0.025

Figure S5. Temporal trends of average prey density in the environment where fish (surviving and dead) dwelled throughout the non-egg stages displayed by release location. Values are shown for the RCP4.5 (left column) and RCP8.5 (right column) emission scenarios. Information from different oceanographic models was combined to estimate temporal trends.

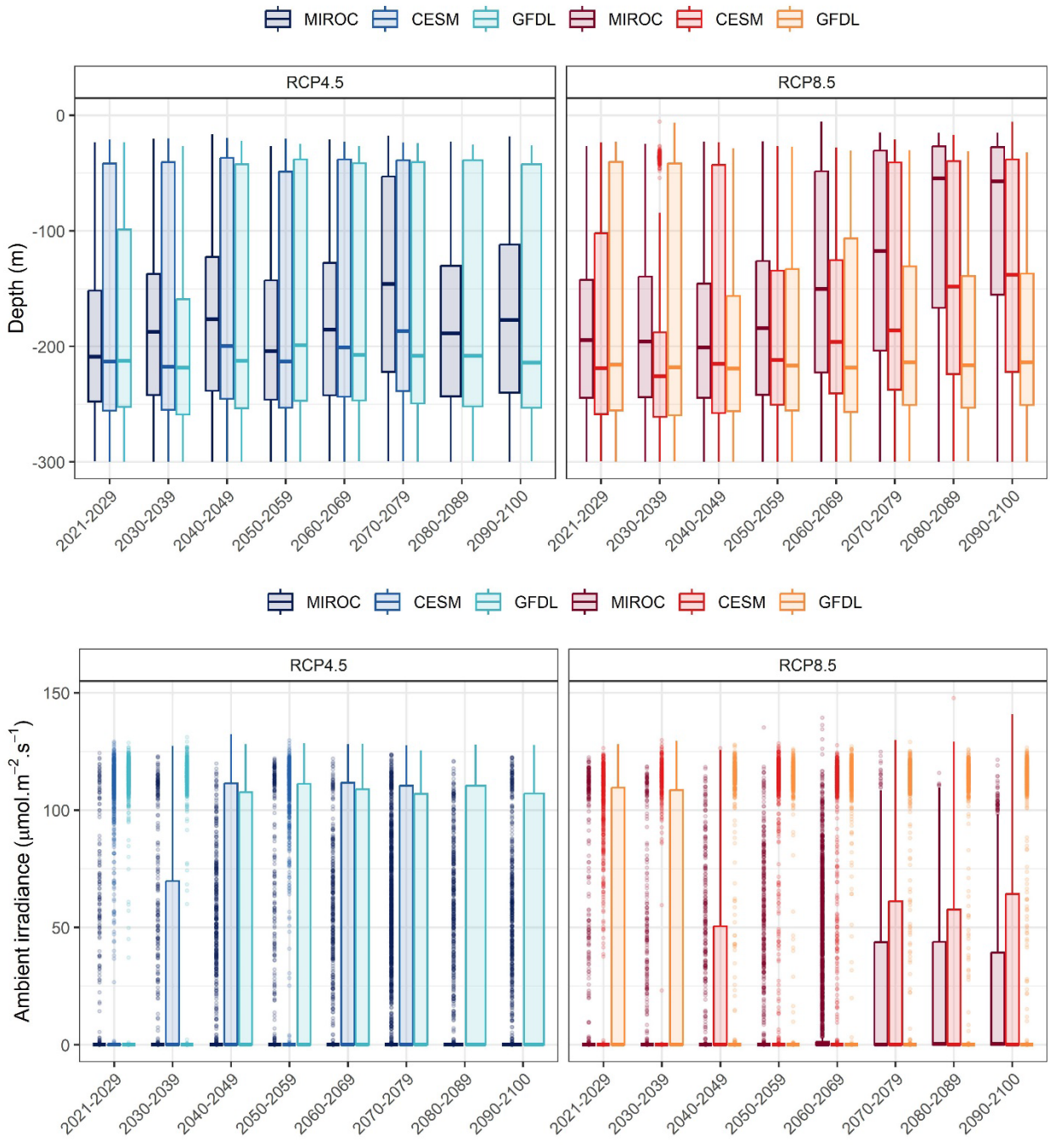

Figure S6. Average depth and ambient light irradiance throughout the lifespan of fish that died from starvation by emission scenario and oceanographic model.

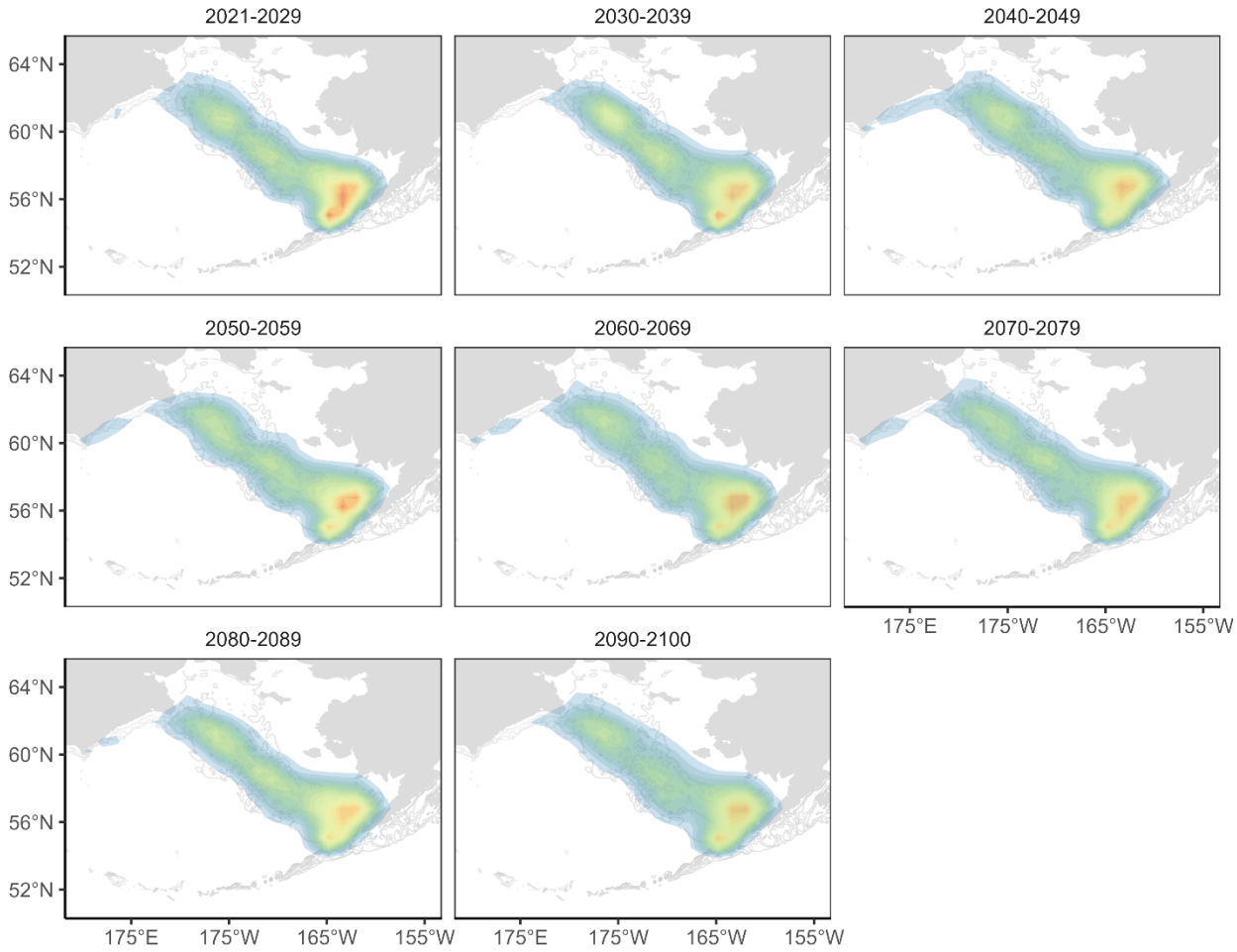

Figure S7. Spatial density of final locations (September 15) by decade for the RCP4.5 emission scenario. Information from different oceanographic models was combined. Red and blue colours indicate higher and lower densities, respectively.

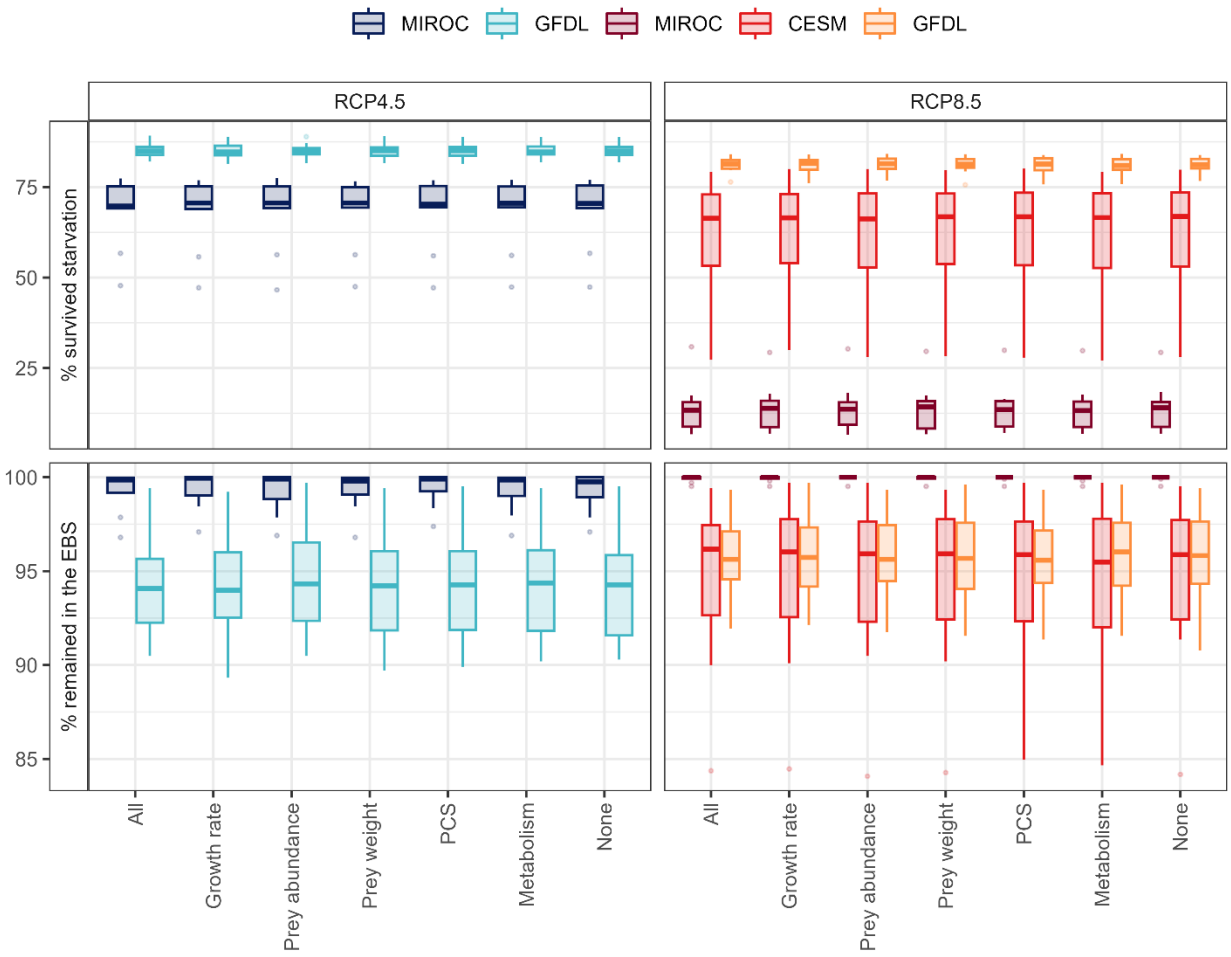

Figure S8. Sensitivity analysis of the impacts of ocean acidification assumed in this study. Percentage of fish that survived to September 15, separated by death cause, only for last decade (2090-2100). All = include the impacts of ocean acidification on all variables, None = no impact of ocean acidification on any variable. No statistical differences (KS test) were found among assumed impacts (p-value > 0.1).

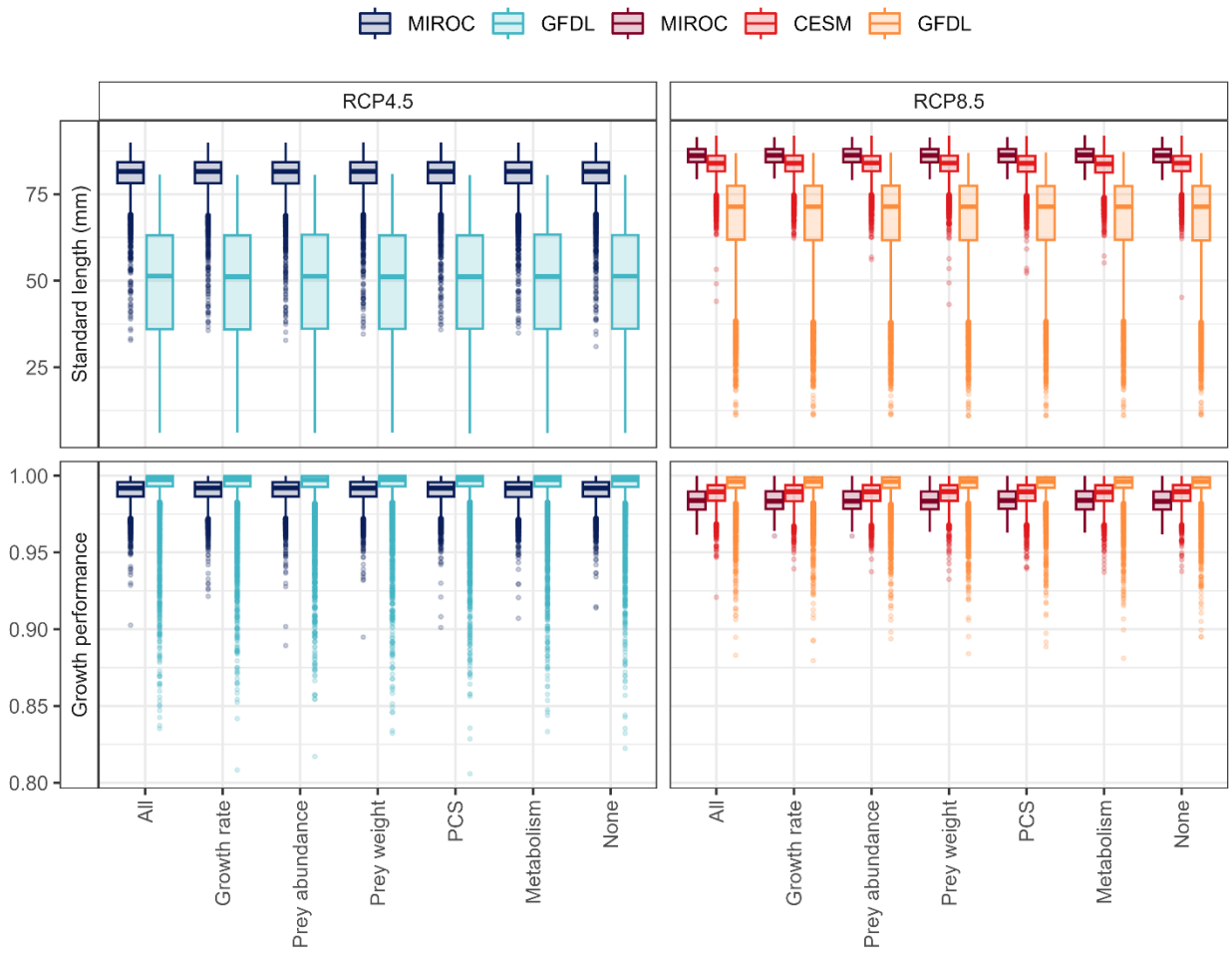

Figure S9. Sensitivity analysis of the impacts of ocean acidification assumed in this study. Standard length and growth performance for surviving fish, only for the last decade (2090-2100). All = include the impacts of ocean acidification on all variables, None = no impact of ocean acidification on any variable. No statistical differences (KS test) were found among assumed impacts (p-value > 0.1).

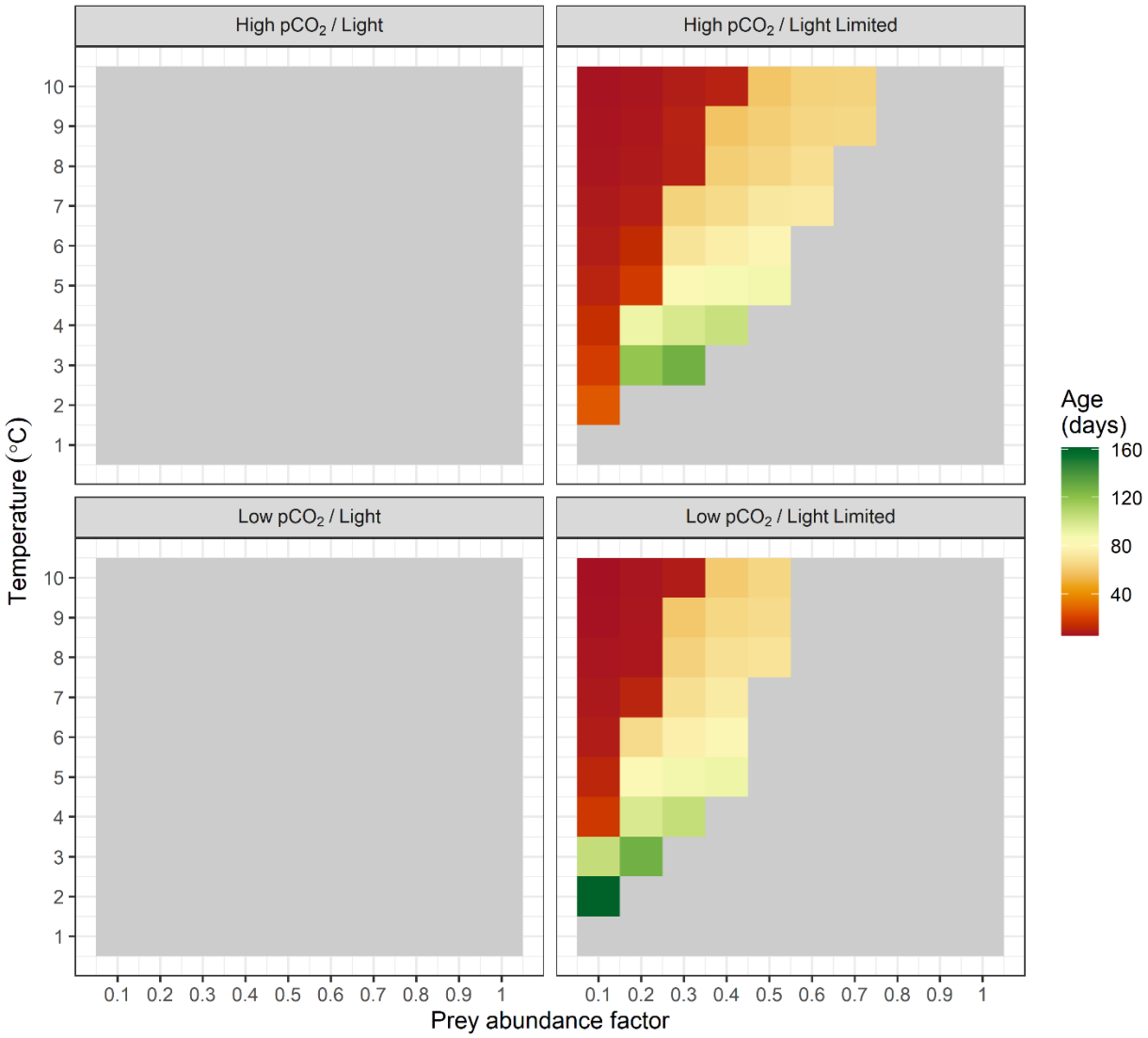

Figure S10. Impacts of low (500 μatm) and high (1500 μatm) pCO_2 on the number of days to die from starvation of a larva dwelling in a fixed environment with hypothetical conditions. 'Light' = environment with high light intensity, 'Light limited' = environment with low light intensity. Gray grids are combinations where the larva survived 165 days. The prey abundance factor multiplies a standard vector of prey densities: Euphausiids = 5.5 mgC/m^3, On-shelf large-bodied copepods = 1.5 mgC/m^3, Off-shelf large-bodied copepods = 1 mgC/m^3, Small-bodied copepods = 4 mgC/m^3.

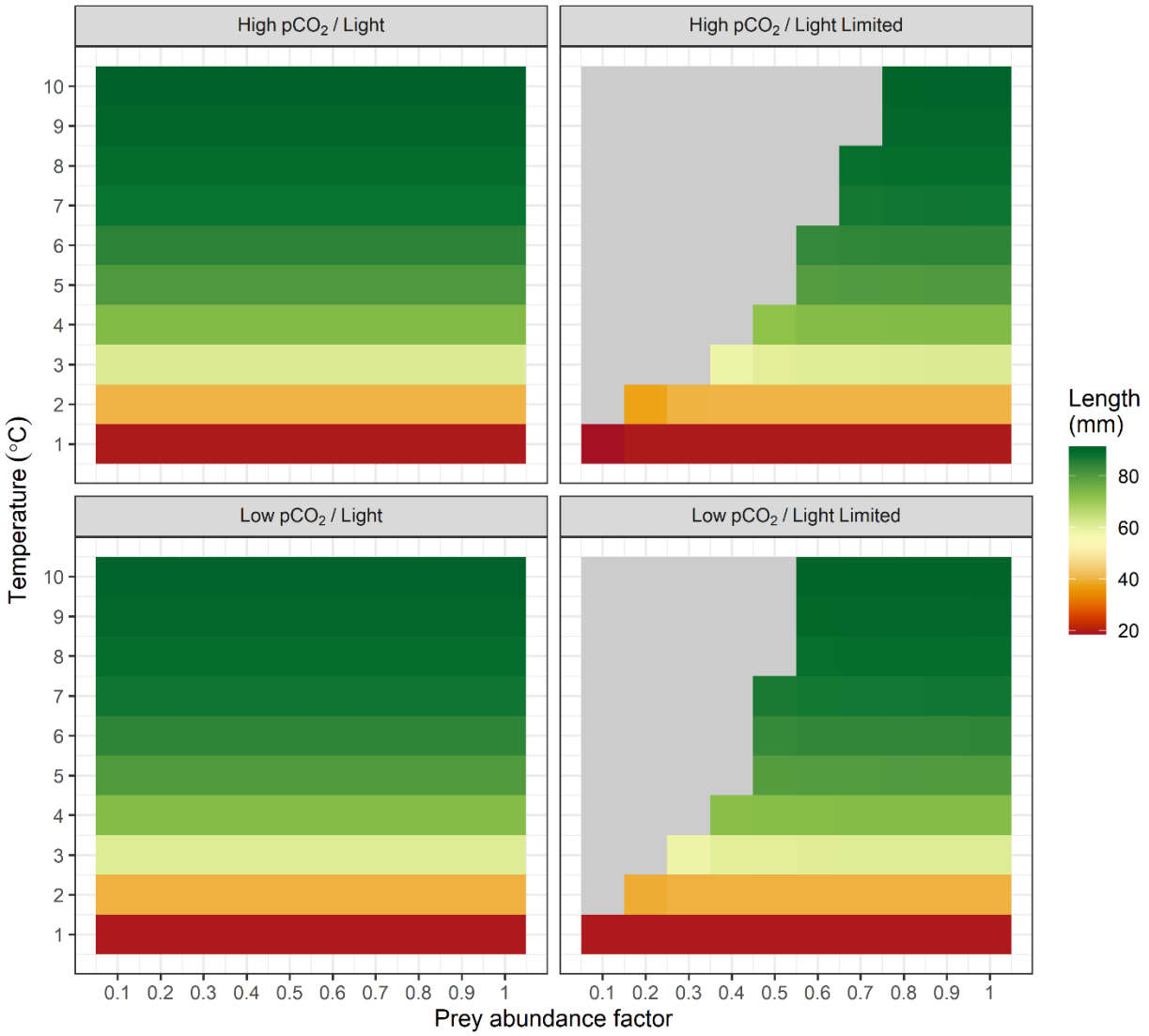

Figure S11. Impacts of low (500 μatm) and high (1500 μatm) pCO_2 on the final standard length (165 days) of a larva dwelling in a fixed environment with hypothetical conditions. 'Light' = environment with high light intensity, 'Light limited' = environment with low light intensity. Gray grids are combinations where the larva died from starvation. The prey abundance factor multiplies a standard vector of prey densities: Euphausiids = 5.5 mgC/m^3, On-shelf large-bodied copepods = 1.5 mgC/m^3, Off-shelf large-bodied copepods = 1 mgC/m^3, Small-bodied copepods = 4 mgC/m^3.

References

Becker, K.N., Warren, J.D., 2014. Material properties of Northeast Pacific zooplankton. ICES Journal of Marine Science 71, 2550–2563. https://doi.org/10.1093/icesjms/fsu109

Harding, G., 1977. Surface Area of the Euphausiid Thysanoessa raschii and Its Relation to Body Length, Weight, and Respiration. J. Fish. Res. Broad Can. 34, 225–231. https://doi.org/10.1139/f77-033

Liu, H., Hopcroft, R.R., 2008. Growth and development of Pseudocalanus spp. in the northern Gulf of Alaska. Journal of Plankton Research 30, 923–935. https://doi.org/10.1093/plankt/fbn046

Liu, H., Hopcroft, R.R., 2007. A comparison of seasonal growth and development of the copepods Calanus marshallae and C. pacificus in the northern Gulf of Alaska. Journal of Plankton Research 29, 569–581. https://doi.org/10.1093/plankt/fbm039

Liu, H., Hopcroft, R.R., 2006. Growth and development of Neocalanus flemingeri/plumchrus in the northern Gulf of Alaska: validation of the artificial-cohort method in cold waters. Journal of Plankton Research 28, 87–101. https://doi.org/10.1093/plankt/fbi102

Saunders, R.A., Rasmussen, J., Tarling, G.A., Brierley, A.S., 2013. Distribution, population dynamics and growth rates of Thysanopoda acutifrons, Thysanoessa inermis and Nematobrachion boöpis in the Irminger Sea, North Atlantic. J. Mar. Biol. Ass. 93, 1287–1301. https://doi.org/10.1017/S0025315412001385

Silva, T., Gislason, A., Astthorsson, O.S., Marteinsdóttir, G., 2017. Distribution, maturity and population structure of Meganyctiphanes norvegica and Thysanoessa inermis around Iceland in spring. PLoS ONE 12, e0187360. https://doi.org/10.1371/journal.pone.0187360